10.1002/chem.201903981

WILEY-VCH

Rhodium Complexes in P–H Bond Activation Reactions

Víctor Varela-Izquierdo,[a] Ana Mª Geer,*[b] Bas de Bruin,[c] José A. López,[a] Miguel A. Ciriano,[a] and Cristina Tejel*[a]

Abstract: The feasibility of oxidative-addition of the P–H bond of $PHPh_2$ to a series of rhodium complexes to give mononuclear hydrido-phosphanido complexes has been analyzed. Three main scenarios have been found depending on the nature of the L ligand added to $[Rh(Tp)(C_2H_4)(PHPh_2)]$: i) clean and quantitative reactions to terminal hydrido-phosphanido complexes $[RhTp(H)(PPh_2)(L)]$ (L = PMe_3, PMe_2Ph and $PHPh_2$), ii) equilibria between Rh(I) and Rh(III) species: $[RhTp(H)(PPh_2)(L)] \leftrightarrows [RhTp(PHPh_2)(L)]$ (L = $PMePh_2$, PPh_3) and iii) a simple ethylene replacement to give the rhodium(I) complexes $[Rh(\kappa^2\text{-}Tp)(L)(PHPh_2)]$ (L = NHCs-type ligands). The position of the P–H oxidative addition-reductive elimination equilibrium is mainly determined by sterics influencing the entropy contribution of the reaction. If ethylene was used as ligand, the unique rhodaphosphacyclobutane complex $[Rh(Tp)(\eta^1\text{-}Et)(\kappa^{C,P}\text{-}CH_2CH_2PPh_2)]$ was obtained. DFT-calculations revealed that the reaction proceeds via a rate limiting oxidative-addition of the P–H bond, followed by a low barrier sequence of reaction steps involving ethylene insertion into the Rh–H and Rh–P bonds. In addition, oxidative-addition of the P–H bond in $OPHPh_2$ to $[Rh(Tp)(C_2H_4)(PHPh_2)]$ gave the related hydride complex $[RhTp(H)(PHPh_2)(POPh_2)]$, but ethyl complexes resulted from hydride insertion into the Rh-ethylene bond in the reaction with $[Rh(Tp)(C_2H_4)_2]$.

Introduction

P–H bond activation at a single metal center is a critical step in metal-catalyzed transformations involving the formation of P–C and P–P bonds, such as hydrophosphanation, hydrophosphonylation, dehydrocoupling, and polymerization reactions.[1] In this reaction, the P–H bond transforms into a terminal phosphanido ligand (M–P) thus enhancing its nucleophilic character and consequently its reactivity.[2]

Among the different approaches to this reaction, one of the most popular involves proton transfer from phosphanes or phosphane oxides to an internal base, i.e. a proton acceptor group coordinated to the metal. Relevant examples include protonolysis at alkyl,[3] and acetate palladium complexes,[4] nickel silanolates[5] and silylamides[6], and iron complexes with an $Fe–CH_2SiMe_3$ motif.[7] In addition, metals with formal d^0 electron count such as lanthanides, early transition metals and some actinides engage in σ-bond metathesis as reported for complexes with alkyls,[8] silylamides,[9] amides,[10] and more recently alkoxy groups.[11]

Moreover, P–H bond activation through metal–ligand cooperation has been recently reported for ruthenium and iridium complexes bearing carbene-type ligands,[12] whereas chelated assisted P–H bond cleavage has been described for diphosphane-phosphane oxides,[13] and diphosphane-phosphane compounds,[14] which results in a phosphanido functionality embedded within a tripodal ligand.

Another interesting methodology that does not require any previous functionalization of the metal centre is the oxidative-addition reaction, i.e., insertion of the metal into a P–H bond, which eventually results in hydrido-phosphanido compounds. However, isolated complexes from such reactions have only been reported in a few instances. As a matter of fact, pioneering work from Schunn[15] and Ebsworth,[16] showed the preparation of iridium(III) complexes derived from the oxidative-addition of PH_3, whereas diphenylphosphane has been successfully added to iridium(I) complexes only recently.[17] Moreover, tri-coordinated complexes of platinum(0)[18] and nickel(0)[19] react with secondary phosphanes to render mononuclear complexes with a $H–M–PR_2$ moiety. However, a similar reaction with a related nickel(I) complex bearing a β-diketiminato ancillary ligand stops at the coordination level, simply leading to $[Ni(nacnac)(PHPh_2)]$.[20] Furthermore, the strong influence of the ancillary ligands in the course of the reactions is evidenced by the reaction of $[Pt(PEt_3)_3]$ with $PHPh_2$, which gives di- and tri-nuclear hydrido-complexes with phosphanido bridging ligands.[21] In these circumstances, the reactivity of the phosphanido ligand is considerably reduced because of the lack of lone electron pairs on the phosphorus atom. This undesirable situation can be avoided by using bulky ligands, as observed in the reaction of $[Co(dtbpe)(C_2H_4)]$ (dtbpe = 1,2-bis(di-tert-butylphosphano)ethane) with 2,6-dimesitylphenylphosphane ($DmpPH_2$), which gives [Co(dtbpe)(H)(PHDmp)].[22]

Hydrido-phosphanido complexes of early and middle transition metals have also been prepared from oxidative-addition reactions of the coordinative- and electronically unsaturated complex $[Ta(^tBu_3SiO)_3]$,[23] and also from electronically saturated complexes $[Mo(Cp^*)(Cl)(N_2)(PMe_3)_2]$,[24] and $[W(dppe)_2(N_2)_2]$[25] with $HPPh_2$. The later require light irradiation to dissociate dinitrogen and thus generate the required coordination vacancy.

[a] V. Varela, Dr. J. A. López, Prof. Dr. M. A. Ciriano, Dr. C. Tejel
Departamento de Química Inorgánica
Instituto de Síntesis Química y Catálisis Homogénea (ISQCH),
CSIC-Universidad de Zaragoza
Pedro Cerbuna 12, 50009-Zaragoza (Spain)
E-mail: ctejel@unizar.es
[b] Dr. A. M. Geer
Department of Chemistry
University of Virginia
Charlottesville, Virginia 22904 (United States)
[c] Prof. Dr. B. de Bruin
University of Amsterdam
Van 't Hoff Institute for Molecular Sciences
Science park 904, 1098 XH Amsterdam (The Netherlands)

Supporting information for this article is given via a link at the end of the document.

There are few examples of P–H bond activation with rhodium complexes. Particularly pertinent to the present work are the rhodium(III) hydrido-phosphanido intermediates observed by Tilley[26] in the synthesis of dinuclear bis(phosphanido) bridged complexes and a rhodium(V) bis(hydrido-phosphanido) complex proposed by Brookhart in the catalytic dehydrocoupling of secondary phosphanes.[27] More recently, Grützmacher reported a terminal rhodium(I)-phosphanido complex with a bulky tetradentate ligand, which contains an unusually long Rh–P bond,[28] whereas we have isolated mononuclear hydrido-phosphanido rhodium complexes and demonstrated that they are intermediates in catalytic hydrophosphanation and dehydrocoupling reactions.[29]

In this paper we showcase the feasibility for the oxidative-addition reaction of the P–H bond of $PHPh_2$ and $OPHPh_2$ to a series of rhodium complexes that give cleanly new mononuclear hydrido-phosphanido complexes, a rhodaphosphacyclobutane complex or ethyl complexes depending on the ancillary ligands and reaction conditions. Some clues to account for the different reactivity observed, supported by DFT-studies are also provided.

Results and Discussion

Reactions with PMe_3, PMe_2Ph and $PHPh_2$

We have previously reported that upon addition of diphenylphosphane to $[Rh(Tp)(C_2H_4)_2]$ (**1**; Tp = hydridotris(pyrazolyl)borate) one ethylene ligand is replaced to give $[Rh(Tp)(C_2H_4)(PHPh_2)]$ (**2**), which was isolated as a yellow microcrystalline solid in excellent yield (Scheme 1).[29] Complex **2** was fully characterized as a species with *TBPY-5* geometry with a non-rotating ethylene at the equatorial position. Slow addition of $PHPh_2$ under vigorous stirring is required to obtain pure samples of complex **2**; otherwise this compound is contaminated with variable amounts of the dinuclear complex $[\{(Tp)(H)Rh(\mu\text{-}PPh_2)\}_2]$ (**3**) (see below) (Scheme 1).

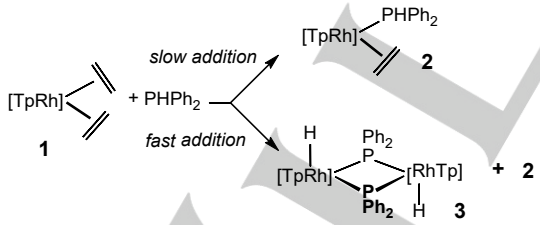

Scheme 1. Reaction of **1** with $PHPh_2$.

Addition of P-donor ligands such as PMe_3, PMe_2Ph, and even $PHPh_2$ to **2** promotes oxidative-addition of the P–H bond to give the hydrido-phosphanido complexes $[Rh(Tp)(H)(L)(PPh_2)]$ (L = PMe_3 **4**, PMe_2Ph **5**, and $PHPh_2$ **6**). These reactions were found to be immediate and quantitative by ^1H and $^{31}P\{^1H\}$ NMR,[29] and complexes **5-6** have now been isolated as yellow microcrystalline solids after workup (Scheme 2).

These complexes represent the first isolated terminal phosphanido rhodium complexes resulting from the formal oxidative addition of a P–H bond to a rhodium center. According to the formulation, complex **6** can be directly prepared by adding two molar equiv. of $PHPh_2$ to the bis(ethylene) complex **1**.

Complexes **4** and **5** were characterized in solution as single static species by the signal of the hydride ligand at high field (δ = –15.62 and –15.44 ppm, respectively) in their ^1H NMR spectra and two doublets of doublets for the two inequivalent phosphorus atoms in the $^{31}P\{^1H\}$ NMR spectra. Interestingly, the values of J(P,Rh) for the terminal phospanido ligand (63 and 62 Hz) were found to be smaller than those corresponding to the phosphane ligands (136 and 138 Hz). It can be attributed to a substantial reduction in the σ–orbital character of the Rh–PR_2 bond as compared to the Rh–phosphane,[17a] and thus provides a useful tool for the identification of the terminal phosphanide ligand.

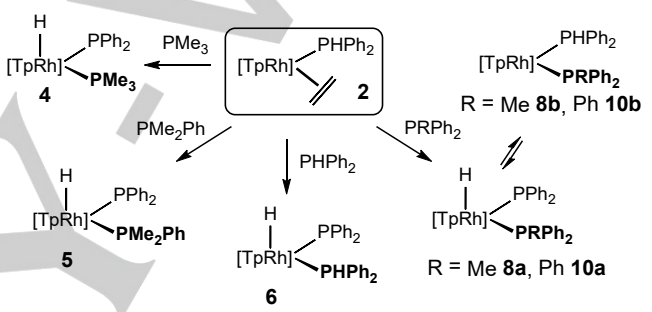

Scheme 2. Synthesis of complexes **4**-**6**, **8** and **10** through P–H bond activation reactions.

Complex **6** proved to be a fluxional species, since a single resonance ($^{31}P\{^1H\}$ NMR) and broad signals (^1H NMR) were observed at room temperature, but it gives sharp NMR signals at –70 ºC in $[D_8]$-toluene. The most relevant resonances at this temperature were the hydride ligand (δ = –14.79 ppm) and the P–H proton (δ = 6.46 ppm) showing a large J(H,P) = 391.0 Hz coupling in the ^1H NMR spectrum.

This fluxionality can be ascribed to a prototropic shift of the PH proton from the phosphane to the phosphanido and, in good agreement; a low barrier transition state of +16.7 kcal mol^{-1} for this shift was calculated with DFT-methods (Figure 1).

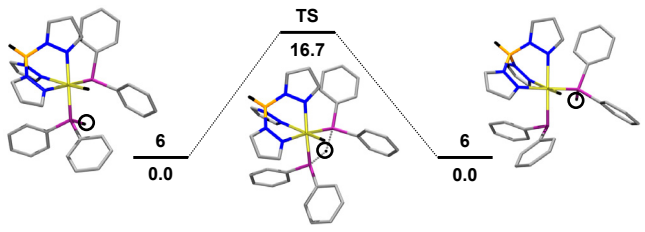

Figure 1. Energy profile (B3LYP-D3, 6-311G(d,p)/LanL2TZ(f)) for the shift of the PH proton from one phosphorus atom to the other in complex **6**. ΔG values in kcal mol^{-1}.

Complex **6** contains an intact diphenylphosphane ligand that could be appropriate for the study of the oxidative-addition reaction of the P–H bond in the presence of a second rhodium center. A bimetallic system might work more efficiently for bond activation due to the cooperation of two metal centers.[30] However, on mixing equimolar amounts of [Rh(Tp)(H)(PHPh$_2$)(PPh$_2$)] (**6**) and [Rh(Tp)(C$_2$H$_4$)$_2$] (**1**) the immediate formation of [Rh(Tp)(C$_2$H$_4$)(PHPh$_2$)] (**2**) was observed instead. Simultaneously, the bis(hydrido) dinuclear complex [{(Tp)(H)Rh(μ-PPh$_2$)}$_2$] (**3**) separated from the reaction media as an insoluble pale-yellow solid.

Complex **3** was characterized by analytical and spectroscopic data. Thus, the equivalent phosphanido bridges gave a triplet due to the coupling to the equivalent ^{103}Rh rhodium nuclei (J(P,Rh) = 92 Hz) in the ^{31}P{^{1}H} NMR, whereas the hydride is observed as a doublet of triplets (^2J(H,P) = 22.3, J(H,Rh) = 17.8 Hz) at δ = –12.54 ppm in the ^{1}H NMR spectrum.

With this experiment in mind, it is easy to understand the strong influence of the experimental procedure on the preparation of complex [Rh(Tp)(C$_2$H$_4$)(PHPh$_2$)] (**2**). Indeed, a fast addition of PHPh$_2$ to [Rh(Tp)(C$_2$H$_4$)$_2$] (**1**) produces a high local concentration of the phosphane, suitable to render complex **6** and then the bis(hydride) dinuclear complex [{(Tp)(H)Rh(μ-PPh$_2$)}$_2$] (**3**) by reaction with unreacted complex **1**.

In addition, solutions of complex **6** in [D$_6$]-benzene transform slowly but quantitatively into the mixed-valence Rh(III)/Rh(I) dinuclear complex [(Tp)(H)Rh^{III}(μ-PPh$_2$)$_2$Rh^{I}(PHPh$_2$)$_2$] (**7**) (Scheme 3).

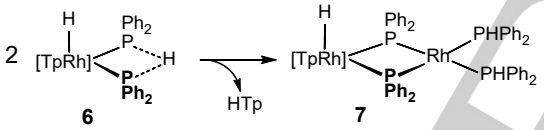

Scheme 3. Synthesis of complex **7**.

This reaction occurs with the concomitant extrusion of one Tp ligand as HTp (^{1}H NMR evidence). On a preparative scale, **7** was isolated as an orange microcrystalline solid in good yield after workup.

The molecular structure of **7**, displayed in Figure 2, shows two rhodium atoms bridged by two phosphanide ligands. The Rh(III) atom, labelled as Rh1, completes a distorted octahedral geometry with the three N-atoms of the Tp and the hydride ligand, whereas the Rh(I) center, labelled as Rh2, shows a square-planar environment with four P-atoms (two from the phosphanide bridges and two from two diphenylphosphane ligands). The Rh1–P1 and Rh1–P2 bond distances are slightly shorter than the related Rh2–P1 and Rh2–P2, which is expected from the different oxidation states Rh1 (Rh^{III}) and Rh2 (Rh^{I}). The long Rh1,Rh2 distance of 3.6298(7) Å excludes any rhodium-rhodium interaction. On the whole, its molecular structure is quite similar to that of the related complex [(Tp)(H)Rh^{III}(μ-PPh$_2$)$_2$Rh^{I}(PHPh$_2$)(PMe$_3$)], previously reported.[29]

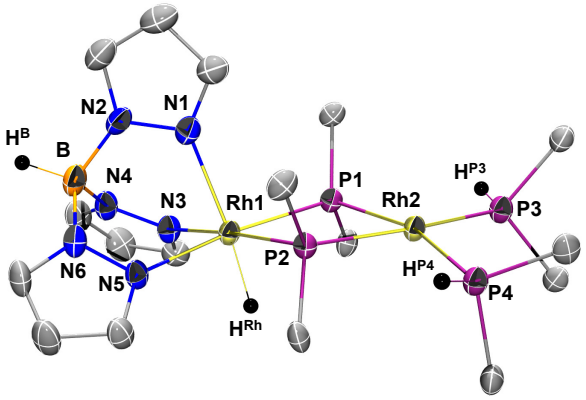

Figure 2. Molecular structure (ORTEP, ellipsoids set at 50% probability) of complex [(Tp)(H)Rh^{III}(μ-PPh$_2$)$_2$Rh^{I}(PHPh$_2$)$_2$] (**7**). Selected bond distances [Å] and angles [°]: Rh1–P1 2.291(1), Rh1–P2 2.274(1), Rh1–N1 2.173(3), Rh1–N3 2.150(3), Rh1–N5 2.133(3), Rh1–H^{Rh} 1.550(1), Rh2–P1 2.338(1), Rh2–P2 2.321(1), Rh2–P3 2.288(1), Rh2–P4 2.276(1), P1-Rh1–N5 172.8(8), P2–Rh1–N3 172.5(9), N1–Rh1–H^{Rh} 174.0(15), P1–Rh2–P4 162.7(4), P2–Rh2–P3 167.6(4). Only the C^{ipso} atoms of the phenyl groups are shown for clarity.

Spectroscopic data of **7** in [D$_6$]-benzene agree with the structure found in the solid state. Thus, the ^{1}H NMR spectrum showed the hydride ligand at δ = –11.45 ppm (td, ^2J(H,P) = 22.4, J(H,Rh) = 18.3 Hz), whereas the equivalent P–H protons produce a doublet of doublets at δ = 5.92 ppm; the large coupling constant J(H,P) = 347.2 Hz agrees with both protons directly bonded to the respective phosphorus atoms. In addition, the ^{31}P{^{1}H} showed two resonances at δ = 13.6 (P^A) and –81.7 (P^B) ppm from a AA'MM'XY spin system (A, A' = PHPh$_2$; M, M'= PPh$_2$, X, Y = ^{103}Rh). The high-field shift of the signal from the phosphanide ligands is in agreement with its bridging position between two rhodium atoms without a metal-metal bond.[31]

Complex **7** is a rare example of a dinuclear bis(phosphanido) mixed-valent compound with a Rh(I),Rh(III) core. Whereas there are several complexes of rhodium with two phosphanido bridges and the metal centers in the same oxidation state,[32] there are limited examples of dirhodium mixed-valent bis(phosphanido) complexes. Nocera *et. al.* described a series of Rh$_2$(II,0)[33] complexes with an octahedral Rh(II) and trigonal bipyramidal Rh(0) and Meek *et. al*. reported a Rh(I,–I) complex with a square planar Rh(I) center and a tetrahedral Rh(–I) center.[34]

Reactions with PMePh$_2$ and PPh$_3$

Interestingly, the reaction of [Rh(Tp)(C$_2$H$_4$)(PHPh$_2$)] (**2**) with the slightly less basic and more sterically demanding phosphane PMePh$_2$ resulted in an equilibrium distribution of the rhodium(III) species [Rh(Tp)(H)(PMePh$_2$)(PPh$_2$)] (**8a**) and the rhodium(I) species [Rh(κ^2-Tp)(PMePh$_2$)(PHPh$_2$)] (**8b**) in solution, which are formed in a 70:30 ratio at room temperature (Schemes 2 and 4). This ratio corresponds to a value of K_{eq} = 2.33 (**8b** ⇆ **8a**) and ΔG_{298} = –0.50 kcal mol^{-1}.

In addition, small amounts of [Rh(Tp)(H)(PHPh$_2$)(PPh$_2$)] (**6**) and [Rh(κ^2-Tp)(PMePh$_2$)$_2$] (**9**) were also involved in the

equilibrium (Scheme 4). They are the result of a phosphane exchange reaction undergone by the rhodium(I) complex **8b**.

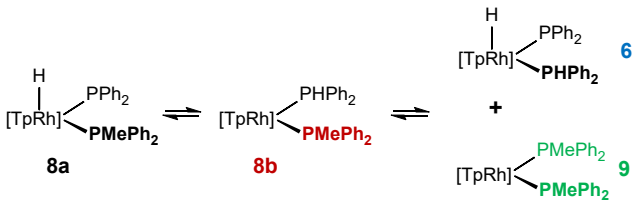

Scheme 4. Equilibrium between complexes **8a**, **8b**, **6,** and **9**.

Such equilibria were easily detected from the ^{1}H,^{1}H-noesy spectrum (Figure 3) because of the chemical exchange of the hydride ligand in **7a** and the PH proton of **8b** (left) as well as that of the methyl group of $PMePh_2$ in complexes **8a**, **8b,** and **9** (right).

From these solutions a yellow solid (**8**) was isolated after workup in very good yield. The IR (ATR) spectrum shows bands at 2457 and 2082 cm^{-1}, assignable to the B–H and Rh–H stretching vibrations, respectively, so most probably complex **8** is the hydrido-phosphanido complex **8a** in the solid state.

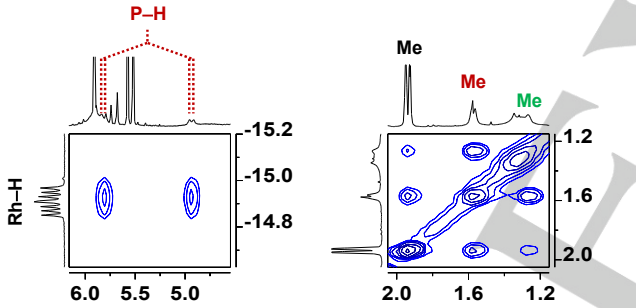

Figure 3. Two selected regions of the ^{1}H,^{1}H-noesy spectrum of **8** showing the negative cross-peaks due to the chemical exchange. Color code: [Rh(Tp)(H)($PMePh_2$)(PPh_2)] (**8a**, black), [Rh(κ^2-Tp)($PMePh_2$)($PHPh_2$)] (**8b**, red) and [Rh(κ^2-Tp)($PMePh_2$)$_2$] (**9**, green).

A similar result occurred on addition of triphenylphosphane to [Rh(Tp)(C_2H_4)($PHPh_2$)] (**2**). Thus, monitoring the reaction by NMR spectroscopy, the complexes [Rh(Tp)(H)(PPh_3)(PPh_2)] (**10a**), [Rh(κ^2-Tp)(PPh_3)($PHPh_2$)] (**10b**), [Rh(Tp)(H)($PHPh_2$)(PPh_2)] (**6**) as well as [{(Tp)(H)Rh(μ-PPh_2)}$_2$] (**3**), [Rh(Tp)(C_2H_4)(PPh_3)] and free PPh_3 were identified in solution (see Supporting Information). In this case, complexes **10a**/**10b** were found to be in a 28:72 ratio at room temperature, which corresponds to a value of Keq = 0.39 (**10b** ⇆ **10a**) and ΔG_{298} = +0.56 kcal mol^{-1}.

DFT-calculations (B3LYP-D3, 6-311G(d,p)/LanL2TZ(f)) on the rhodium(I) complexes [Rh(κ^2-Tp)(L)($PHPh_2$)] (L = PMe_2Ph **8b**, PPh_3 **10b**) showed that they are square-planar species with the Tp ligand bonded to rhodium in a κ^2-fashion and with the six-membered metallacycle Rh(N-N)$_2$B showing a boat conformation (Figure 4).

This puckered structure leads to two conformers depending on the location of the uncoordinated pyrazolate ring, either inside or outside the pocket of the complex. Both conformers were clearly observed in the ^{31}P{^{1}H} NMR spectra at –60 ºC for **8b** and **10b** and the equilibrium between them accounts for the intriguing spectra at room temperature where only one signal of the phosphorus atoms of **8b** and **10b** was clearly observed, whereas the second one is very broad and hard to distinguish from the baseline (Figure 4).

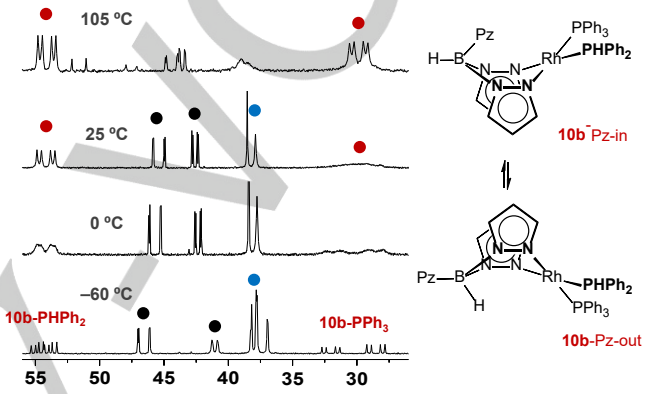

Figure 4. Selected region of the VT-^{31}P{^{1}H} NMR spectra of the reaction [Rh(Tp)(C_2H_4)($PHPh_2$)] (**2**) with PPh_3 in [D_8]-toluene showing conformers **10b**-Pz-in and **10b**-Pz-out. Color code: [Rh(Tp)(H)(PPh_3)(PPh_2)] (**10a**, black), [Rh(Tp)(PPh_3)($PHPh_2$)] (**10b**, red) and [Rh(Tp)(H)($PHPh_2$)(PPh_2)] (**6**, blue).

Comments on phosphane ligands promoting P–H bond activation reactions.

At first glance, one could argue that the oxidative-addition reaction of the P–H bond in complexes [Rh(κ^2-Tp)(L)($PHPh_2$)] would be favored by increasing the electron density at the rhodium center. As the electron richness of the metal in this series is given by the donor ability of the ligand L, this magnitude can be evaluated from the ν(CO) stretching frequencies in complexes that only differ in the L ligand. For such purpose, the complexes [Rh(acac)(CO)(L)] (acac = acetylacetonate) that show a unique ν(CO) band were chosen.[35] The observed frequencies, collected in Table 1, give the following order of electron density: PMe_3 > PMe_2Ph > $PMePh_2$ > PPh_3> $PHPh_2$, which fit fairly well with the TEPs (Tolman Electronic Parameters) previously reported.[36]

From these data is clear that electronic effects are not the most relevant factor to account for the above described results. In particular, the richest (PMe_3) and poorest ($PHPh_2$) rhodium centers give both the corresponding rhodium(III) hydrido-phosphanido complexes cleanly. In both cases, the reactions were found to be almost instantaneous, achieving completion in less than 5 min.

Table 1. IR ν(CO) band in cm^{-1} for the rhodium(I) complexes [Rh(acac)(CO)(L)] in toluene and computed cone angles (°).[37]

	PMe_3	PMe_2Ph	$PMePh_2$	PPh_3	$PHPh_2$
ν(CO)	1968	1971	1975	1980	1982
Cone angles	118	122	136	145	128

Interestingly, a nice fit is found if steric effects are considered instead. Indeed, the order according to the cone angle: PMe_3 < PMe_2Ph < $PHPh_2$ < $PMePh_2$ < PPh_3 (Table 1) fit very well with the observed reactivity. Hydrido-phosphanido complexes were obtained for PMe_3, PMe_2Ph and $PHPh_2$, whereas with the bigger ligands, $PMePh_2$ and PPh_3, the equilibrium [Rh(κ^2-Tp)(L)($PHPh_2$)] ⇆ [Rh(Tp)(H)(L)(PPh_2)] was observed. In other words, it can be concluded that an increase in the size of the ligand diminishes the stability of the rhodium(III) oxidation state relative to the rhodium(I) counterpart, in such a way that an equilibrium between them is observed.

Since for complexes with the phosphanes $PMePh_2$ and PPh_3 both species are clearly observable by NMR, the thermodynamic parameters for the P–H oxidative-addition reactions:

[Rh(κ^2-Tp)(L)($PHPh_2$)] ⇆ [Rh(Tp)(H)(L)(PPh_2)]

could be estimated from the Van 't Hoff plots (see Supporting Information). In both cases, a straight line was obtained giving values of ΔH = –2.12±0.2 (**8**), –2.64±0.1 (**10**) kcal mol^{-1} and ΔS = –5.77±0.6 (**8**), –10.74±0.5 (**10**) u.e, which lead to ΔG at 298 K of –0.40 (**8**) and +0.56 (**10**) kcal mol^{-1}.

Although both reactions are exothermic, with similar values of enthalpy, the entropic contribution, more negative for the more steric demanding ligand (PPh_3), is the key factor that determines the lower stability of the rhodium(III) hydrido-phosphanido complex. Indeed, the change in the environment of rhodium, from square-planar to octahedral –associated to the P–H bond activation reaction– produces more crowded complexes, which are more destabilized as the size of the ligand increases. Accordingly, complexes with the less demanding ligands PMe_3, PMe_2Ph and $PHPh_2$ are expected to be obtained as hydrido-phosphanido complexes as observed experimentally.

Reactions with N-heterocyclic carbenes

The ability of N-heterocyclic carbenes to promote P–H bond activation reactions was also tested by reacting [Rh(Tp)(C_2H_4)($PHPh_2$)] (**2**) with IMes (1,3-dimesitylimidazol-2-ylidene) and BzIMe (1,3-dimethylbenzyimidazol-2-ylidene). The products from the reactions were found to be the rhodium(I) complexes [Rh(κ^2-Tp)(L)($PHPh_2$)] (L = IMes **11**, BzIMe **12**), which were isolated as yellow solids in good yields (Scheme 5).

Analytical and spectroscopic data of **11**-**12** agree with the proposed formulation. In particular, the PH proton was observed as a doublet of doublets at δ = 5.95 (**11**) and 6.16 (**12**) ppm with large J(P,H) = 332.5 and 322.7 Hz and small ^2J(H,Rh) = 3.3 and 1.1 Hz couplings constants, respectively, at low temperature. In addition, the abnormally large J(P,Rh) coupling constants of 195 and 192 Hz, respectively, have to be related with an square-planar environment of rhodium, further confirmed by a X-ray diffraction study of complex **11**. Moreover, complex **11** was found to adopt the boat conformation in the solid state, with the uncoordinated pyrazolate ring dangling outside the pocket of the complex (**11**-Pz-out, Figure 5).

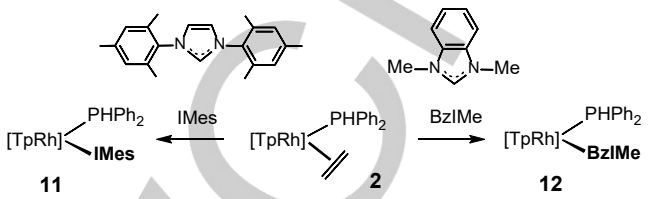

Scheme 5. Reactions of [Rh(Tp)(C_2H_4)($PHPh_2$)] (**2**) with IMes and BzIMe.

DFT-calculations (B3LYP-D3, 6-311G(d,p)/LanL2TZ(f)) on the conformer found in the solid state (**11**-Pz-out) as well as on that with the pyrazolate ring inside the pocket of the complex (**11**-Pz-in) revealed the former to be more stable than the later by 3.9 kcal mol^{-1}. On the contrary, for complex **12** having the less demanding BzIMe ligand, the conformer **12**-Pz-in was found to be more stable than **12**-Pz-out by 4.1 kcal mol^{-1}.

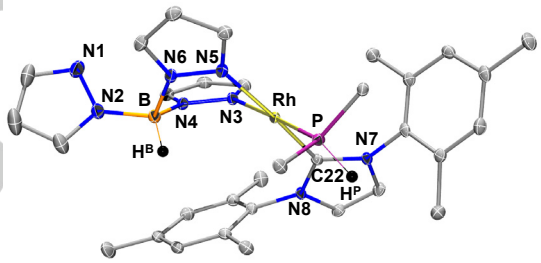

Figure 5. Molecular structure (ORTEP, ellipsoids set at 50% probability) of complex [Rh(κ^2-Tp)(IMes)($PHPh_2$)] (**11**-Pz-out). Selected bond distances [Å] and angles [°]: Rh–P 2.1985(5), Rh–N3 2.0957(14), Rh–N5 2.1014(14), Rh–C22 1.9903(16), P-Rh–N3 176.64(4), N5–Rh–C22 173.78(6).

Complexes, **11** and **12**, were found to be fluxional species in solution. The analysis of the ^{1}H,^{1}H-noesy spectrum of **11** at room temperature revealed the presence of a dynamic process in which the three pyrazolate rings, the four methyl groups at the *ortho* position of the IMes ligand, and the phenyl groups of the $PHPh_2$ exchange. This process is slightly faster in the case of complex **12**, since at this temperature the ^{1}H NMR spectrum is close to that expected for the fast-exchange region. Such exchange could take place through the participation of pentacoordinated *TBPY-5* species (the turnstile motion), as generally admitted in Tp-complexes.[38] However, in the particular case of complex **11**, first a boat-to-boat inversion of the six-membered metallacycle Rh(N-N)$_2$B is required to achieve the suitable conformer (**11**-Pz-in) to undergo κ^2-κ^3 isomerism.

The lack of a further P–H bond oxidative addition in the case of complexes **11** and **12** cannot be attributed to electronic effects

as commented before. Indeed, they contain the more donating ligands (NHCs), with ν(CO) stretching frequencies in the complexes [Rh(acac)(CO)(L)] (L = IMes, BzIMe) of 1955 and 1962 cm^{-1}, respectively. Most probably, the particular steric requirements of these ligands that place the steric demand in a specific direction account for their lack of further reactivity.

Reaction with ethylene

Warming a solution of [Rh(Tp)(C_2H_4)($PHPh_2$)] (**2**) in the presence of ethylene (6 bar) at 60 ºC for six days resulted in the novel rhodaphosphacyclobutane complex [Rh(Tp)(η^1-Et)($\kappa^{C,P}$-$CH_2CH_2PPh_2$)] (**13**, Scheme 6), which was isolated as an orange microcrystalline solid in good yields.

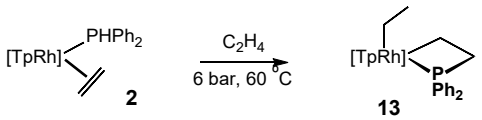

Scheme 6. Synthesis of the rhodaphosphacyclobutane complex **13** from **2**.

Control of the temperature and pressure of ethylene is crucial to get pure samples of **13** in such a way that complex **13** was contaminated with variable amounts of [{(Tp)(H)Rh(μ-PPh_2)}$_2$] (**3**) under lower pressures of ethylene and/or higher temperatures. As an example, this reaction was completed in 3 h at 105 ºC in d^8-toluene under an atmosphere of ethylene (2 bar), but the yield in **13** decreased up to 45%.

Complex **13** was identified as the rhodaphosphacyclobutane compound shown in Scheme 6 by its analytical and spectroscopic data. Thus, the ^{1}H NMR spectrum showed the diastereotopic CH_2 protons of ethyl group as two multiplets coupled to a triplet corresponding to the methyl group (Figure 6, in blue). In addition, the large coupling constant of the methylenic carbon to rhodium (*J*(C,Rh) = 24 Hz) clearly evidences the presence of a direct Rh–C bond.[39]

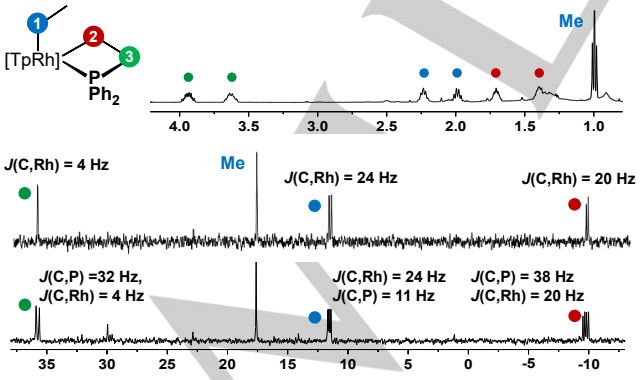

Figure 6. Selected regions of the ^{1}H (top), ^{13}C{^{1}H,^{31}P} (middle), and ^{13}C{^{1}H} (bottom) NMR spectra of complex **13**.

Signals due to the protons and carbons of the rhodaphosphacyclobutane moiety were clearly identified in the ^{1}H, ^{13}C{^{1}H}, and ^{13}C{^{1}H,^{31}P} NMR spectra (red and green, Figure 6). The methylenic protons and carbon directly attached to rhodium (H_2C^2, in red) were high-field shifted relative to that bonded directly to phosphorus (H_2C^3, in green). In particular, the signal at δ= –9.5 ppm, with a large coupling constant to rhodium of 20 Hz, can be attributed to the CH_2 group directly attached to the rhodium atom (C^2), whereas that at δ = 36.0 ppm (^{2}*J*(C,Rh) = 4 Hz) corresponds to C^3 directly bonded to phosphorus. A characteristic feature of the rhodaphosphetane moiety was present in the ^{31}P{^{1}H} NMR spectrum, which showed a doublet at δ= –36.1 ppm (*J*(P,Rh) = 122 Hz) shifted upfield in *ca.* 70 ppm relative to **2** (48.1 ppm). Such a shift is diagnostic of a phosphorus atom in a four-membered metallacycle.[40]

Repetitive attempts to grow single crystals of complex **13** under different conditions gave systematically very small and geminated microcrystals, preventing thus a further crystallographic structure determination. Hence, we resorted to DFT geometry optimization to get structural information. An energy minimum was found for [Rh(Tp)(η^1-Et)($\kappa^{C,P}$-$CH_2CH_2PPh_2$)] (**13'**) (Figure 7), with rhodium in an almost octahedral environment. The strong trans influence of the alkyl carbons (C1 and C2) is clearly demonstrated by the considerable elongation of the Rh–N1 and Rh–N5 bond distances (2.240 and 2.211 Å, respectively) in comparison with the other Rh–N1 bond (2.118 Å), which is *trans* to the phosphane. The four-membered ring slightly deviates from planarity (P–C–C–Rh torsion angle of 12.55º). Among the endocyclic angles, the P–Rh–C angle is the most acute (71.24º).

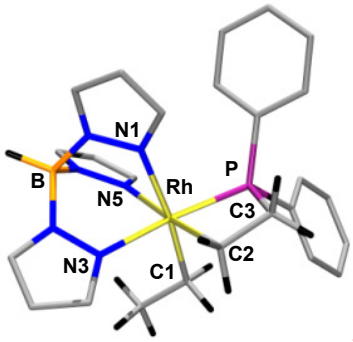

Figure 7. DFT-calculated structure (BP86, def2-TZVP, disp3) of complex [Rh(Tp)(Et)($\kappa^{C,P}$-$CH_2CH_2PPh_2$)] (**13'**).

The formation of the rhodaphosphacyclobutane **13** is remarkable as there are very few examples of metallaphosphacyclobutanes, mainly limited to ruthenium[41] and palladium[42] complexes. Rhodium phosphacyclobutanes are also known, however they have mainly been obtained from *ortho* metalation of phosphanes.[43] To our knowledge, this is the first example of a rhodaphosphacyclobutane derived from an alkene, as well as the first example of insertion of a non-activated olefin (ethylene) into a Rh–P bond. Moreover, reactions leading to P–C bond

formation with unactivated olefins such as ethylene are essentially absent in the literature,[1b,d,f] Notable examples include a nickel phosphanidene complex which can undergo ethylene insertion leading to an organic phosphirane via an intermediate four-membered nickel phosphacycle,[44] the nickel mediated reaction of a primary phosphane to a functionalized phosphane through ethylene insertion,[19] and a ruthenium phosphide species which reacts with olefins, including ethylene and 1-hexene, to yield metallaphosphacyclobutanes.[41]

The most plausible mechanistic pathways to **13** are shown in Scheme 7 and involve two inner-sphere ethylene insertions into the Rh–H and the Rh–P bonds. In both cases, the first step is the oxidative addition of diphenylphosphane to give intermediate **A**. In the next step, insertion of the coordinated ethylene can occur into either the Rh–H (Scheme 7, in green) or the Rh–P bond (Scheme 7, in red). Coordination of ethylene on the resulting intermediates (**B1**/**B2**) would produce **C1**/**C2** suitable for the second ethylene insertion into the Rh–P/Rh–H bonds, respectively.

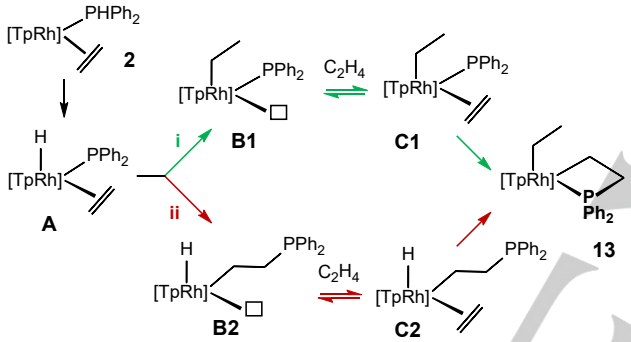

Scheme 7. Plausible mechanistic pathways for the formation of complex **13** from **2**. Path i starts with ethylene insertion into the Rh–H bond, whereas path ii starts with ethylene insertion into Rh–P the bond.

The first step in both pathways is the oxidative addition of the P–H bond of complex **2** to form intermediate **A**. This reaction has a relative high barrier of +28.7 kcal mol^{-1} according to DFT (Figure 8). This seems to be the rate determining step for formation of **13**. Experimentally the reaction requires heating to 60 °C for 6 days to reach completion, from which one can estimate an activation barrier of about +27.3 kcal mol^{-1} using the Eyring equation,[45] which is in reasonable agreement with the slightly overestimated DFT barrier

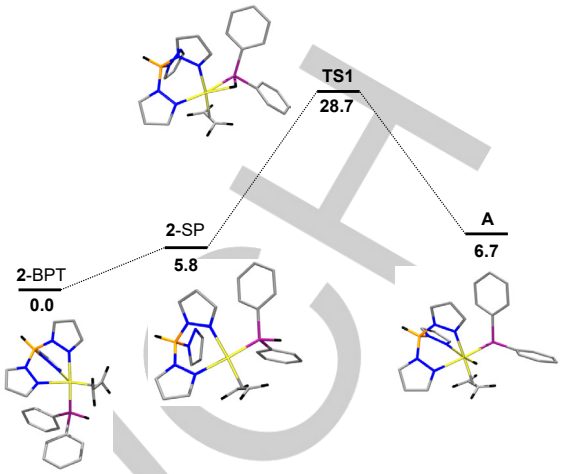

Figure 8. DFT computed (BP86, def2-TZVP, disp3) barrier for oxidative addition of the P–H bond in complex **2** to form intermediate **A**.

The two most logical pathways for formation of complex **13** from **A** were both computed with DFT. The green pathway via intermediates **B1** and **C1** is clearly the preferred pathway, and has low barrier and very accessible transition states once **A** is formed (Figure 9). The alternative red pathway via intermediates **B2** and **C2** has much higher barriers (Figure 10), and formation of intermediate **B2'** from **B2** involving dissociation of the Rh–P bond of the rhodaphosphacyclobutane ring (+31.3 kcal mol^{-1}) is even more endergonic than **TS1** (Figure 8).

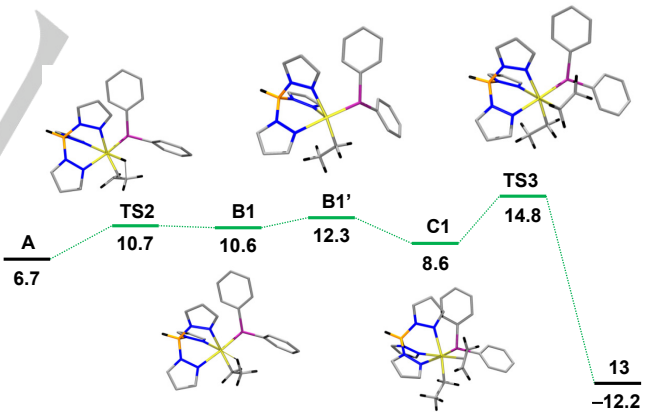

Figure 9. Green pathway: DFT computed (BP86, def2-TZVP, disp3) pathway for formation of complex **13** from intermediate **A** via **B1** and **C1**.

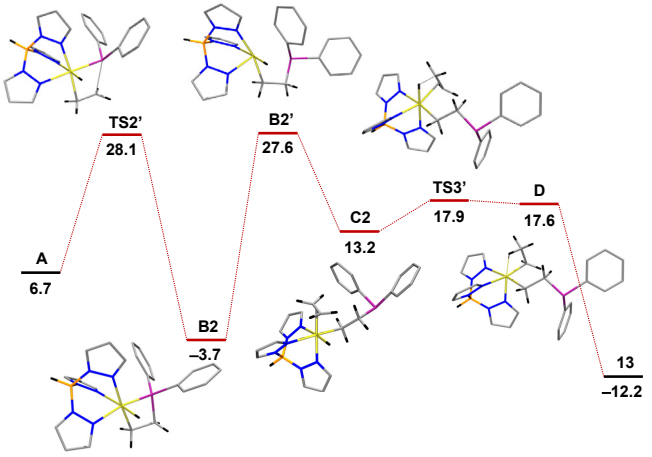

Figure 10. Red pathway: DFT computed (BP86, def2-TZVP, disp3) pathway for formation of complex **13** from intermediate **A** via **B2** and **C2**.

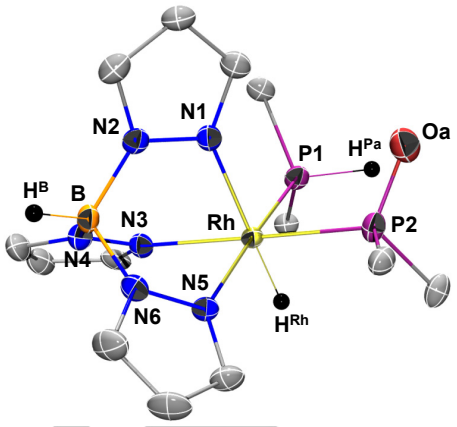

Figure 11. Molecular structure (ORTEP, ellipsoids set at 50% probability) of complex [Rh(Tp)(H)(P(O)Ph_2)(PHPh_2)] (**14**). Selected bond distances [Å] and angles [°] : Rh–P1 2.238(2), Rh–P2 2.268(2), Rh–N1 2.162(4), Rh–N3 2.164(4), Rh–N5 2.122(4), P2–Oa 1.511(6), P1–Rh–N5 174.5(2), P2–Rh–N3 179.0(2), N1–Rh–H^{Rh} 176(3). Only the C^{ipso} of the phenyl rings are shown for clarity.

It is therefore clear that the reaction to form complex **13** should follow the green pathway (via intermediates **B1** and **C1**) as shown in Figure 6. The mechanism described herein is distinct from the ruthenium chemistry described by Rosenberg *et. al*. in that the ruthenium species undergoes a 2+2 cycloaddition through a Ru phosphanidene (Ru=P) intermediate[41] whereas the chemistry reported here occurs through the rhodium hydrido phosphanido intermediate **A**.

Our results indicate a preference for ethylene insertion into the Rh–H bond and are in agreement with related DFT-studies[46] on alkyne insertion into metal-phospanide complexes for which calculations showed that alkyne insertion into a M–H bond should be much easier compared to a M–P bond (M= Pd, Ni, Pt, and Rh).

Attempts to eliminate ethane and PEtPPh_2 from **13** aimed to close a hypothetical dual hydrophosphanation/hydrogenation catalytic cycle were tested using HPPh_2 as proton source. Therefore, complex **13** was warmed in the presence of PHPh_2 (20 mol equiv.) at 80 ºC under an atmosphere of ethylene (6 bar). PEtPPh_2 (20 %) and ethane were observed as products, but the major component of the reaction mixture was found to be Ph_2P–PPh_2 (80%), the product from the dehydrocoupling reaction. Even after prolonged heating of **13** (105 ˚C for a week) no evidence for ethylene deinsertion was observed. Other ligands were also added to **13** to favor reductive elimination. However, no reaction was observed with CO (1 atm., 80 ˚C, 48 h) by ^{1}H and ^{31}P NMR spectroscopy.

Reactions with OPHPh_2

Diphenylphosphane oxide reacts with [Rh(Tp)(C_2H_4)(PHPh_2)] (**2**) to give [Rh(Tp)(H)(POPh_2)(PHPh_2)] (**14**), which was fully characterized by analytical and spectroscopic methods, including a X-ray crystallographic study (Figure 11).

Its molecular structure shows the rhodium atom in the center of a slightly distorted octahedron bound to the three nitrogen atoms of the Tp ligand, two phosphorus atoms coming from the phosphanido and the phosphane oxide respectively, and the hydride ligand. The remaining proton is bound to a P-atom, as deduced by its signal at δ = 7.17 ppm (J(H,P) = 410.2, ^2J(H,Rh) = 10.5 Hz) in the ^{1}H NMR spectrum, but it could not be located in the structure due to the disorder of the oxygen atom over the two phosphorus atoms (75.3(14)% and 24.7(14)% relative abundance).

Spectroscopic data of **14** in solution agreed with the structure shown in Figure 11. Thus, the ^{31}P{^{1}H} NMR spectrum showed two doublets of doublets at δ = 75.7 and 33.5 ppm; the peak at high-field has been assigned to the phosphane PHPh_2 ligand. The hydride ligand resonates at δ = –13.74 as a ddd by coupling to the two *cis* P-atoms (^2J(H,P) = 23.2 and 20.4 Hz) and to the ^{103}Rh nuclei (^1J(H,Rh) = 16.0 Hz), whereas the P–H proton was observed at δ = 7.17 ppm in the ^{1}H NMR spectrum. Moreover, ^{1}H,^{31}P-hmbc NMR experiments (with J(H,P) = 10 and 400 Hz) showed that this proton was strongly coupled to the phosphane ligand (J(H,P) = 410.1) and in less extension to the POPh_2 ligand (J(H,P) = 10.5 Hz). These observations along with its molecular structure (Figure 11, in which both P-atoms are coordinated to rhodium) definitively confirms that the hydride ligand comes from the phosphane oxide (OPHPh_2) instead of the phosphane PHPh_2.

A plausible sequence of reactions in the synthesis of **14** is shown in Scheme 8. The red pathway starts with the coordination of diphosphane oxide to render intermediate **A**, followed by the activation of P–H bond. This step requires decoordination of one of the pyrazolate arms to allow the approaching of the P–H bond to rhodium. The participation of the tautomer hydroxydiphenylphosphane would give intermediate **B** followed by an easy O–H bond activation reaction (green pathway). Although both possibilities could be

operative, we believe that the pathway marked in green is more plausible, in spite of the smaller abundance of the hydroxy tautomer in the equilibrium,[47] because of the type of bonds involved. Indeed, such activations through the tautomer phosphinous acid have been previously proposed for ruthenium complexes on the basis of DFT-calculations.[12]

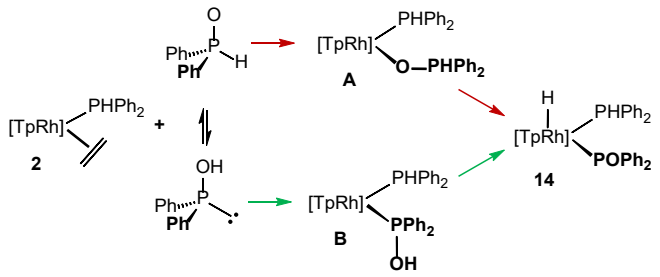

Scheme 8. Plausible sequence of reactions for the synthesis of **14** from **2** and $OPHPh_2$.

Interestingly, the reaction of $OPHPh_2$ with the bis(ethylene) complex $[Rh(Tp)(C_2H_4)_2]$ (**1**) (in 1:1 molar-ratio) did not give the mononuclear complex $[Rh(Tp)(C_2H_4)(OPHPh_2)]$ (analogous to **2**), but the bis(η^1-ethyl) dinuclear complex $[\{(Tp)(\eta^1\text{-Et})Rh(\mu\text{-}OPPh_2)\}_2]$ (**15**) along with the mononuclear complexes $[Rh(Tp)(\eta^1\text{-R})(POPh_2)(POHPh_2)]$ (R = Et,**16** and H, **17**) (Scheme 9). From these solutions, complex **15** was isolated after working up, whereas a mixture of complexes **16** and **17** was isolated in high yield if solutions of **15** in the presence of two molar equiv. of $OPHPh_2$ were warmed for 14 h at 60 ºC in toluene.

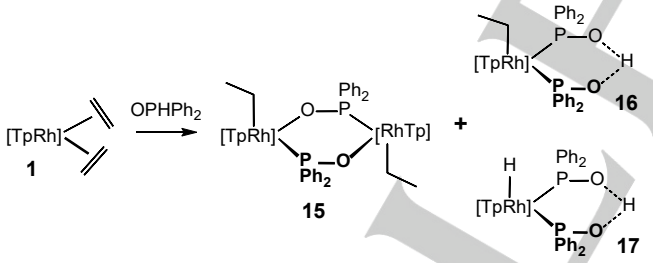

Scheme 9. Reaction of **1** with $OPHPh_2$.

The dinuclear nature of **15** is evident from the $^{31}P\{^1H\}$ NMR, which shows a multiplet corresponding to the AA' part of an AA'XX' spin system (A, A' = ^{31}P; X, X' = ^{103}Rh) for the two equivalent P-nuclei. The ethyl group was clearly observed as three signals (1:1:3 ratio) in the ^1H NMR spectrum with the methylenic protons strongly coupled to the phosphorus atom according to the $^1H,^{31}P$-hmbc spectrum.

Complexes **16** and **17** could not be separated because of their high tendency to crystallize together in a disordered manner. Indeed, all single crystals studied by X-ray methods revealed that they contained both complexes in an approximate 1:1 ratio.[48] Nonetheless, spectroscopic data of the isolated solid agrees with a mixture of **16** and **17** in a 2:1 molar ratio. Thus, a broad signal, corresponding to the hydrogen interacting with the two oxygens, was found at δ = 18.34 ppm in the ^1H NMR spectrum. The methylenic protons of the ethyl ligand in **16** were observed at δ = 2.22 ppm as a qtd because of the coupling with the three protons of the adjacent methyl group (^3J(H,H) = 7.5 Hz), the two equivalent phosphorous atoms (^3J(H,P) = 4.1 Hz) and ^{103}Rh (^2J(H,Rh) = 1.9 Hz). The hydride ligand in **17** was detected at δ = –12.99 ppm as a td because of the coupling with the two equivalent phosphorus atoms (^2J(H,P) = 21.7 Hz) and 103-rhodium (J(H,Rh) = 16.7 Hz).

Scheme 10 shows a plausible sequence of reactions that accounts for the synthesis of **15**-**17** from the reactions of $[Rh(Tp)(C_2H_4)_2]$ (**1**) with $OPHPh_2$. The first part of the reaction would consist in the coordination of the hydroxydiphenyl tautomer to give intermediate **A**, followed by the oxidative-addition reaction of the O–H bond to give species **B**, as previously commented for complex **14**.

From **B**, ethylene replacement by a new molecule of $OPHPh_2$ would give the hydride complex $[Rh(Tp)(H)(POPh_2)(POHPh_2)]$ (**17**), but a competitive insertion reaction of the hydride ligand into the Rh–ethylene bond would give to intermediate **C**. From **C**, a dimerization would render the dinuclear complex $[\{(Tp)(\eta^1\text{-Et})Rh(\mu\text{-}OPPh_2)\}_2]$ (**15**), whereas coordination of $OPHPh_2$ would produce the mononuclear complex $[Rh(Tp)(\eta^1\text{-Et})(POPh_2)(POHPh_2)]$ (**16**).

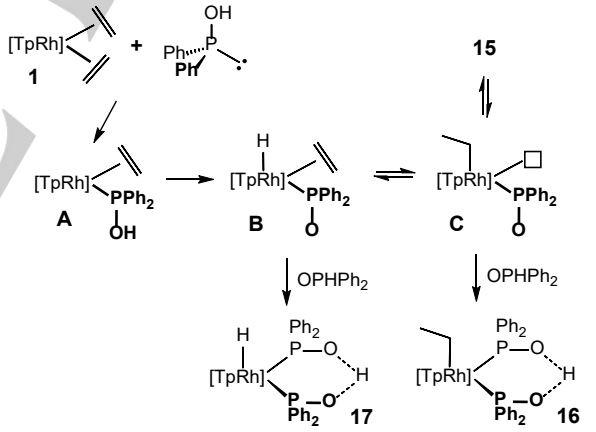

Scheme 10. Plausible sequence of reactions to complexes **15**-**17**.

The proposed equilibrium between complex **15** and intermediates **B** and **C** has been verified by the reaction of **15** with $OPHPh_2$ (in 1:2 molar ratio), which systematically gives a mixture of the mononuclear complexes **16** and **17** in a 2:1 ratio. Since no change of this ratio was observed on warming this mixture for prolonged time, complexes **16** and **17** are not in equilibrium and, most probably, they arise from intermediates **B** and **C**, respectively. This ratio could represent the relative rates for $OPHPh_2$ coordination to **B**/**C** (assuming a fast equilibrium **B** ⇆ **C**) or alternatively the ratio of **B** and **C** in the equilibrium if coordination of $OPHPh_2$ were faster. However, taking into

account the low ΔG values for hydride insertions into Rh–ethylene bonds,[49] the first possibility seems to be more plausible.

Summary and conclusions

Combination of tridentate hydridotrispyrazolylborate and phosphane ligands on rhodium provides an useful platform for the selective oxidative-addition reaction of the P–H bond in diphenylphosphane to give the new hydrido-phosphanido complexes [Rh(Tp)(H)(L)(PPh_2)] (L = PMe_3, PMe_3Ph, $PHPh_2$). Increasing the steric bulk of the phosphane by using $PMePh_2$ or PPh_3 also results in the corresponding hydrido-phosphanido complexes, but in this case they stablish an equilibrium with the corresponding square-planar rhodium(I) complexes with a κ^2-coordinated Tp ligand. The thermodynamic parameters for such equilibria: [Rh(κ^2-Tp)(L)($PHPh_2$)] ⇆ [Rh(Tp)(H)(L)(PPh_2)] (L = $PMePh_2$, PPh_3), obtained from the Van't Hoff plots, indicate both reactions to be slightly exothermic (ΔH = –2.12±0.2 and –2.64±0.1 kcal mol^{-1}) with a negative entropic contribution; larger for the bulkier PPh_3 than for $PMePh_2$ (ΔS = –10.74±0.5 and –5.77±0.6 u.e., respectively). These results strongly support that steric factors, over electronic effects, govern the formation of the final products. Indeed, the richest (with PMe_3) and poorest (with $PHPh_2$) rhodium centers give both the corresponding rhodium(III) hydrido-phosphanido complexes cleanly. However, complexes with the highly donating NHCs ligands IMes and BzIMe remained in the rhodium(I) oxidation state under similar conditions. In this case, the lack of reactivity can be attributed to the particular steric requirements of these ligands that direct the steric demands in a specific direction, hindering access to the P–H bond activation transition state.

The reaction of [Rh(Tp)(C_2H_4)($PHPh_2$)] with diphenylphosphane under an ethylene atmosphere leads to the the unique rhodaphosphacyclobutane complex [Rh(Tp)(η^1-Et)($\kappa^{C,P}$-$CH_2CH_2PPh_2$)]. It is the result of a double ethylene insertion into the Rh–H and Rh–P bonds. Computational studies provided insights into the reaction mechanism, revealing that the lowest energy pathway involves oxidative addition of the P–H bond in **2** to form intermediate **A**, followed by a low barrier reaction steps sequence involving ethylene insertion into the thus formed Rh–H and Rh–P bonds.

A formal P–H bond activation of phosphane oxide also takes place to give the related hydrido complex [RhTp(H)($PHPh_2$)($POPh_2$)], in the reaction of [Rh(Tp)(C_2H_4)($PHPh_2$)] with $OPHPh_2$, but ethyl complexes result from hydride insertion into Rh-ethylene bond in the reaction with [Rh(Tp)(C_2H_4)$_2$]. In these reactions, the participation of the phosphinous acid tautomer is proposed, firstly coordinating to the metal though the P-atom, and then transferring the O–H proton to rhodium.

We believe that the results reported here expand the knowledge on oxidative-addition reactions of secondary phosphanes to rhodium, which can be useful for the design of catalysed processes leading to green syntheses of phosphanes.

Experimental Section

All of the operations were carried out under an argon atmosphere using standard Schlenk techniques as well as dry-box facilities. The complexes [Rh(Tp)(C_2H_4)$_2$] (**1**),[38, 50] [Rh(Tp)(C_2H_4)($PHPh_2$)] (**2**),[29] and [Rh(Tp)(H)(PMe_3)(PPh_2)] (**4**)[29] were prepared according to literature methods. Diphenylphosphane purchased from Aldrich was found to contain ca. 4% of diphenylphosphane oxide. The oxide was removed by silica gel column chromatography using diethyl ether as eluent. Diethyl ether was then evaporated under vacuum. Carbon, hydrogen, and nitrogen analyses were carried out with a Perkin-Elmer 2400 CHNS/O microanalyzer. Mass spectra and high resolution mass specta of complexes were acquired on a Bruker Esquire3000 plus (ESI+) and a Bruker MicroTOF-Q (ESI+) spectrometers, respectively. NMR spectra were recorded on Bruker AV300, AV400 and AV500 spectrometers operating at 300.13, 400.13 MHz and 500.13 MHz, respectively, for ^{1}H. Chemical shifts are reported in ppm and referenced to $SiMe_4$, using the internal signal of the deuterated solvent (^{1}H and ^{13}C) and external H_3PO_4 85% in water (^{31}P) and HBF_4•OEt_2 15% in [D_6]-benzene (^{11}B). IR spectra of solid samples were recorded with a Perkin-Elmer 100 FT-IR spectrometer (4000−400 cm^{-1}) equipped with attenuated total reflectance (ATR). For the labeling of protons and carbons see the Supporting Information.

Synthesis of the complexes. [{(Tp)(H)Rh(μ-PPh_2)}$_2$] (3). An NMR tube was charged with [Rh(Tp)(C_2H_4)$_2$] (**1**, 9.0 mg, 0.024 mmol) and [Rh(Tp)(H)($PHPh_2$)(PPh_2)] (**6**, 16.6 mg, 0.024 mmol) and then [D_6]-benzene (0.5 mL) was added. The reaction was monitored by ^{1}H and ^{31}P{^{1}H} NMR showing the immediate formation of [Rh(Tp)(C_2H_4)($PHPh_2$)] (**2**) while a white solid corresponding to complex **3** precipitated. The resulting suspension was centrifuged, decanted and the remaining solid was washed with hexane (3 x 0.5 mL) and vacuum-dried. Yield: 7.5 mg (62.5 %). IR (ATR): ν (B–H)/cm^{-1} 2485 (m), ν(Rh–H)/cm^{-1} 2064 (m); ^{1}H NMR (400.13 MHz, [D_6]-benzene, 25 ºC): δ = 9.91 (br s, 2H, PPh^{o1}), 7.68 (d, ^3J(H,H) = 2.3 Hz, 2H, Pz^{B5}), 7.52 br s, 2H, PPh^{m1}), 7.38 (dd, ^3J(H,H) = 2.4, ^5J(H,H) = 0.7 Hz, 4H, Pz^{A5}), 7.17 (dd, ^3J(H,H) = 2.4 Hz, 2H, Pz^{B3}), 7.07 (t, ^3J(H,H) = 6.8 Hz, 2H, PPh^{p1}), 7.01 (m, 4H, PPh^{o2}), 6.81 (t, ^3J(H,H) = 7.5 Hz, 2H, PPh^{p2}), 6.76 (br s, 2H, $PPh^{m1'}$), 6.65 (dd, ^3J(H,H) = 2.0, ^4J(H,H) = 0.7 Hz, 4H, Pz^{A3}), 6.64 (br s, 2H, $PPh^{o1'}$), 6.60 (t, ^3J(H,H) = 7.7 Hz, 4H, PPh^{m2}), 5.78 (t, ^3J(H,H) = 2.1 Hz, 2H, Pz^{B4}), 5.67 (t, ^3J(H,H) = 2.2 Hz, 4H, Pz^{A4}), –12.54 (td, ^2J(H,P) = 22.3, J(H,Rh) = 17.8 Hz, 1H, Rh–H); ^{31}P{^{1}H} NMR (161.3 MHz, [D_6]-benzene, 25 ºC): δ = –48.9 (t, J(P,Rh) = 92 Hz); ^{11}B{^{1}H} NMR (128.4 MHz, [D_6]-benzene, 25 ºC): δ = –3.83 (s, BH); anal. calcd. (%) for $C_{42}H_{42}N_{12}B_2P_2Rh_2$ (1004.24): C 50.23, H 4.22, N 16.74; found: C 49.80, H 4.35, N 17.02.

[Rh(Tp)(H)(PMe_2Ph)(PPh_2)] (5). Dimethylphenylphosphane, (25 μL, 0.18 mmol) was added to a yellow solution of [Rh(Tp)(C_2H_4)($PHPh_2$)] (**2**, 94.5 mg, 0.18 mmol) in toluene (4 mL) producing an immediate color change from yellow to orange. After stirring for 10 min, the solution was concentrated to ca. 0.5 mL and precipitated with hexane (6 mL). The orange solid that precipitated was separated by decantation, washed with cold hexane (1 x 2 mL) and vacuum-dried. Yield: 83.4 mg (73 %). IR (ATR): ν(B–H)/cm^{-1} 2460 (m), ν(Rh–H)/cm^{-1} 2142 (m); ^{1}H NMR (500.13 MHz, [D_8]-toluene, 25 ºC): δ = 8.16 (t, ^3J(H,H) = ^3J(H,P) = 6.2 Hz, 2H, PPh^{o1}), 7.57 (d, ^3J(H,H) = 2.1 Hz, 1H, Pz^{B5}), 7.46 (d, ^3J(H,H) = 1.2 Hz, 1H, Pz^{B3}), 7.33 (d, ^3J(H,H) = 2.1 Hz, 1H, Pz^{A5}), 7.26 (br t, ^3J(H,H) = ^3J(H,P) = 2.1 Hz, 1H, Pz^{C5}), 7.23 (m, 4H, PMe_2Ph^o + PPh^{m1}), 7.12 (t, ^3J(H,H) = 7.2 Hz, 1H, PPh^{p1}), 7.10 (br s, 1H, Pz^{C3}), 6.96 (t, ^3J(H,H) = 7.3 Hz, 1H, PMe_2Ph^p), 6.92 (t, ^3J(H,H) = 7.3 Hz, 2H, PMe_2Ph^m), 6.83 (t, ^3J(H,H) = ^3J(H,P) = 7.2 Hz, 2H, PPh^{o2}), 6.81 (hidden, 1H, PPh^{p2}), 6.73 (t, ^3J(H,H) = 7.3, 2H, PPh^{m2}), 6.66 (d, ^3J(H,H) = 2.1 Hz, 1H, Pz^{A3}), 5.96 (t, ^3J(H,H) = 2.0 Hz, 1H, Pz^{B4}), 5.61 (t, ^3J(H,H) = 2.1 Hz, 1H, Pz^{A4}), 5.53 (m, 1H, Pz^{C4}), 4.57 (br d, J(H,B) = 135.1 Hz, 1H, HB), 1.64 (d, J(H,P) = 9.6

Hz, 3H, PMe), 1.45 (d, *J*(H,P) = 9.6 Hz, 3H, PMe), –15.44 (ddd, ^2J(H,P) = 27.1, 9.6 Hz, *J*(H,Rh) = 16.0 Hz, Rh–H); $^{31}P\{^1H\}$ NMR (202.5 MHz, [D_8]-toluene, 25 ºC): δ = 35.4 (dd, *J*(P,Rh) = 62 Hz, ^2J(P,P) = 16 Hz, 1P, PPh_2), 14.5 (dd, *J*(P,Rh) = 138 Hz, ^2J(P,P) = 16 Hz, 1P, PMe_2Ph); $^{11}B\{^1H\}$ NMR (160.5 MHz, [D_8]-toluene, 25 ºC): δ = –3.44 (s, BH); HR-MS *m/z* calcd. for $C_{29}H_{33}BN_6P_2Rh$ [*M*+H]$^+$ 641.1390, found: 641.1397 (error (mD) = –0.7); anal. calcd. (%) for $C_{29}H_{32}N_6BP_2Rh$ (640.27): C 54.40, H 5.04, N 13.13; found: C 54.12, H 4.87, N 12.99.

[Rh(Tp)(H)(PHPh$_2$)(PPh$_2$)] (6). Diphenylphosphane, (26 μL, 0.15 mmol) was added to a yellow solution of [Rh(Tp)(C_2H_4)$_2$] (**1**, 78.8 mg, 0.15 mmol) in toluene (4 mL). An immediate color change to bright orange was observed. After stirring for 10 min, the solution was concentrated to to ca. 0.5 mL and hexane (5mL) was added. The yellow solid that precipitates was separated by decantation and washed with hexane. Yield: 82 mg (81%). IR (ATR): ν(B–H)/cm^{-1} 2462 (m), ν(P–H)/cm^{-1} 2310 (m), ν(Rh–H)/cm^{-1} 2117 (m); ^{1}H NMR (400.13 MHz, [D_8]-toluene, –70 ºC): δ = 8.19 (s, 1H, Pz^{C3}), 8.08 (br s, 2H, PPh^{o1}), 7.75 (br s, 2H, PPh^{o2}), 7.61 (br t, ^3J(H,H) = ^3J(H,P) = 7.4 Hz, 2H, $HPPh^{o1}$), 7.46 (s, 1H, Pz^{B5}), 7.37 (s, 2H, Pz^{A5+C5}), 7.16 (s, 2H, PPh^{m1}), 6.97 (m, 7H, $PPh^{(m+p)2}$ + $HPPh^{(m+p)1}$ + PPh^{p1}), 6.89 (s, 1H, Pz^{A3}), 6.76 (t, ^3J(H,H) = 6.6 Hz, 1H, $HPPh^{p2}$), 6.63 (t, ^3J(H,H) = 6.6 Hz, 2H, $HPPh^{m2}$), 6.53 (t, ^3J(H,H) = ^3J(H,P) = 6.9 Hz, 2H, $HPPh^{o2}$), 6.46 (dd, ^1J(H,P) = 391.0 Hz, ^3J(H,Rh) = 10.0 Hz, 1H, $PHPh_2$), 5.85 (br s, 1H, Pz^{C4}), 5.83 (br s, 1H, Pz^{B3}), 5.63 (br s, 1H, Pz^{B4}), 5.55 (br s, 1H, Pz^{A4}) –14.79 (dt, ^2J(H,P) = 26.8, ^2J(H,P) = *J*(H,Rh) = 13.0 Hz, 1H, Rh–H); $^{31}P\{^1H\}$ NMR (162.0 MHz, [D_8]-toluene, –70 ºC): δ = 37.9 (br d, *J*(P,Rh) = 70 Hz, 1P, PPh_2), 37.1 (br d, *J*(P,Rh) = 143 Hz, 1P, $HPPh_2$); $^{11}B\{^1H\}$ NMR (128.4 MHz, [D_8]-toluene, –70 ºC): δ = –3.77 (s, BH); (s); HR-MS *m/z* calcd. for $C_{33}H_{33}BN_6P_2Rh$ [*M*+H]$^+$ 689.1390, found: 689.1368 (error (mD) = 2.2); anal. calcd. (%) for $C_{33}H_{32}N_6BP_2Rh$ (687.30): C 57.58, H 4.69, N 12.21; found: C 56.95, H 5.05, N 12.64.

[(Tp)(H)Rh^{III}(μ-PPh$_2$)$_2$Rh^{I}(PHPh$_2$)$_2$] (7). Diphenylphospane (19.7 μL, 0.114 mol) was added to a solution of [Rh(Tp)(C_2H_4)($PHPh_2$)] (**2**, 60.5 mg, 0.114 mmol) in toluene (5 mL). After stirring for 3 days, the solution was concentrated to ca. 0.5 mL, layered with hexane (6 mL) and left undisturbed overnight. The orange microcrystals that precipitated were separated by decantation, washed with cold hexane (1 x 2 mL) and vacuum-dried. Yield: 49.1 mg (74%). IR (ATR): ν(B-H)/cm^{-1} 2477 (m), ν(Rh-H)/cm^{-1} 2064(m); ^{1}H RMN (300.13 MHz, [D_6]-benzene, 25 ºC): δ 8.38 (t, ^3J(H,H) = ^3J(H,P) = 7.2, 4H,PPh^{o1}), 8.03 (t, ^3J(H,H) = 7.2 Hz, 4H, PPh^{o2}), 7.37 (d, ^3J(H,H) = 2.1 Hz, 1H, Pz^{B5}), 7.35 (m, 4H, $HPPh^{o1}$), 7.34 (dd, ^3J(H,H) = 2.3 Hz, 2H, Pz^{A5}), 7.07 (d, ^3J(H,H) = 1.8 Hz, 2H, Pz^{A3}), 7.03 (t, ^3J(H,H) = 7.6 Hz, 4H, PPh^{m2}), 6.94 (m, 16H, $HPPh^{o2}$ + PPh^{m1} + PPh^{p2} + $HPPh^{(m+p)1}$), 6.84 (m, 8H, $HPPh^{(m+p)2}$ + PPh^{p1}), 6.14 (d, ^3J(H,H) = 1.9 Hz, 1H, Pz^{B3}), 5.92 (dd, *J*(H,P) = 347.2 Hz, ^2J(H,Rh) = 11.3 Hz, 1H, HP), 5.70 (t, ^3J(H,H) = 2.1 Hz, 2H, Pz^{A4}), 5.47 (t, ^3J(H,H) = 2.1 Hz, 1H, Pz^{B4}), 4.55 (br d, ^1J(H,B) = 130.9 Hz, 1H, HB), –11.45 (td, ^2J(H,P) = 22.4, *J*(H,Rh) = 18.3 Hz, 1H, Rh–H); $^{31}P\{^1H\}$ RMN (121.5 MHz, [D_6]-benzene, 25 ºC): spin system AA'MM'XY (A, A' = $PHPh_2$, M, M' = PPh_2, X, Y = ^{103}Rh); δ(P^A) = 13.6 ppm, δ(P^M) = –81.7 ppm, ^2J(P^A,$P^{A'}$) = 30 Hz, ^2J(P^A,P^M) = 20 Hz, ^2J(P^A,$P^{M'}$) = 265 Hz, ^2J($P^{A'}$,P^M) = 265 Hz, ^2J($P^{A'}$,$P^{M'}$) = 20 Hz, ^2J(P^M,$P^{M'}$) = 100 Hz, J(P^A,$^{A'}$,Rh^X) = 160 Hz, J($P^{M,M'}$,Rh^X) = 120 Hz, J($P^{M,M'}$,Rh^Y) = 100 Hz; $^{11}B\{^1H\}$ RMN (96.3 MHz, [D_6]-benzene, 25 ºC): δ –3.68 (s, BH); HR-MS *m/z* calcd. for $C_{57}H_{54}BN_6P_4Rh_2$ [*M*+H]$^+$ 1163.1567, found: 1163.1610 (error (mD) = –4.3); anal. calcd. (%) for $C_{57}H_{53}N_6BP_4Rh_2$ (1162.59): C 58.89, H 4.60, N 7.23; found: 56.93, H 4.80, N 7.99.

Reaction of [Rh(Tp)(C_2H_4)($PHPh_2$)] (2) with $PMePh_2$. Methyldiphenylphospane (22 μL, 0.11 mol) was added to a solution of [Rh(Tp)(C_2H_4)($PHPh_2$)] (**2**, 57.0 mg, 0.11 mmol) in toluene (5 mL). After stirring for 20 min, the solution was evaporated to ca. 0.5 mL, layered with hexane (6 mL) and left undisturbed overnight. The orange microcrystals that precipitated were separated by decantation, washed with cold hexane (1 x 2 mL) and vacuum-dried. Yield: 60.8 mg (80%). IR (ATR): ν(B–H)/cm^{-1} 2457 (m), ν(Rh–H)/cm^{-1} 2082 (m); HR-MS *m/z* calcd. for $C_{34}H_{35}BN_6P_2Rh$ [*M*+H]$^+$ 703.1547, found: 703.1561 (error (mD) = –1.4); anal. calcd (%) for $C_{34}H_{34}N_6BP_2Rh$ (702.3380): C 58.14, H 4.88, N 11.97; found: C 57.41, H 4.89, N 12.22.

NMR data for [Rh(Tp)(H)($PMePh_2$)(PPh_2)] (**8a**, 70%)**:** ^{1}H NMR (500.13 MHz, [D_8]-toluene, 25 ºC): δ = 8.05 (t, ^3J(H,H) = ^3J(H,P) = 6.3 Hz, 2H, PPh^{o1}), 7.62 (t, ^3J(H,H) = ^3J(H,P) = 7.6 Hz, 2H, $PMePh_2^{o1}$), 7.59 (d, ^3J(H,H) = 1.9 Hz, 1H, Pz^{B5}), 7.46 (br s, 1H, Pz^{B3}), 7.38 (d, ^3J(H,H) = 2.0 Hz, 1H, Pz^{A5}), 7.26 (br t, ^3J(H,H) = ^3J(H,P) = 1.9 Hz, 1H, Pz^{C5}), 7.18 (m, 2H, $PMePh_2^{m1}$), 7.10 (br s, 1H, Pz^{C3}), 7.03 (m, 6H, $PPh^{(m+p)1}$ + $PMePh_2^{o2}$ + $PMePh_2^{p1}$), 6.90 (td, ^3J(H,H) = 7.2, ^4J(H,H) = 1.3 Hz, 1H, $PMePh_2^{p2}$), 6.79 (m, 4H, PPh^{o2} + $PMePh_2^{m2}$), 6.67 (m, 3H, $PPh^{(m+p)2}$), 6.61 (d, ^3J(H,H) = 1.9 Hz, 1H, Pz^{A3}), 5.91 (t, ^3J(H,H) = 2.0 Hz, 1H, Pz^{B4}), 5.57 (t, ^3J(H,H) = 2.0 Hz, 1H, Pz^{A4}), 5.52 (br t, ^3J(H,H) = 1.9 Hz 1H, Pz^{C4}), 4.62 (br d, *J*(H,B) = 128.5 Hz, 1H, HB), 1.94 (d, *J*(H,P) = 9.2 Hz, *J*(H,Rh) = 1.4 Hz, 3H, PMe), –14.90 (ddd, ^2J(H,P) = 24.3, 7.7 Hz, *J*(H,Rh) = 15.0 Hz, 1H, Rh–H); $^{31}P\{^1H\}$ NMR (202.5 MHz, [D_8]-toluene, 25 ºC): δ = 38.6 (dd, *J*(P,Rh) = 65 Hz, ^2J(P,P) = 10 Hz, 1P, PPh_2), 29.6 (dd, *J*(P,Rh) = 141 Hz, ^2J(P,P) = 10 Hz, 1P, $PMePh_2$); $^{11}B\{^1H\}$ NMR (128.4 MHz, [D_8]-toluene, 25 ºC): δ = –3.71 (s, BH).

Selected NMR resonances for [Rh(Tp)($PMePh_2$)($PHPh_2$)] (**8b**, 30%): ^{1}H NMR (400.13 MHz, [D_8]-toluene, 35 ºC): δ = 5.38 (dd, ^1J(H,P) = 352.0, ^3J(H,Rh) = 18.1 Hz, 1H, $PHPh_2$), 1.58 (d, *J*(H,P) = 8.4 Hz, 3H, $PMePh_2$); $^{31}P\{^1H\}$ NMR (161.3 MHz, [D_8]-toluene, 80 ºC): δ = 38.8 (dd, *J*(P,Rh) = 167 Hz, ^2J(P,P) = 60 Hz, 1P, $PMePh_2$), 28.7 (dd, *J*(P,Rh) = 176 Hz, ^2J(P,P) = 60 Hz, 1P, $PHPh_2$); $^{11}B\{^1H\}$ NMR (128.4 MHz, [D_8]-toluene, 25 ºC): δ = –1.66 (s, BH).

[Rh(Tp)($PMePh_2$)$_2$] (9). $PMePh_2$ (96.5 μL, 0.519 mmol) was added to a solution of [Rh(Tp)(C_2H_4)$_2$] (**1**, 96.5 mg, 0.259 mmol) in [D_6]-benzene (0.5 mL). The initial yellow solution inmediately turns to dark yellow. After stirring for 30 min, the solution was concentrated to ca. 0.5 mL and hexane (5 mL) was added. The yellow solid that precipitates was separated by decantation and washed with hexane (2 x 5mL). Yield: 126.4 mg (67%). IR (ATR): ν(B–H)/cm^{-1} 2459 (m). ^{1}H NMR (500.13 MHz, [D_6]-benzene, 25 ºC): δ = 7.84 (br s, 3H, Pz), 7.65 (br s, 8H, $PMePh_2^o$), 6.99 (br, 15H, Pz+ $PMePh_2^{m+p}$), 5.92 (br s, 3H, Pz), 1.29 (td, *J*(H,P) = 3.8 Hz, *J*(H,Rh) = 1.1 Hz, 1H); $^{31}P\{^1H\}$ NMR (202.5 MHz, [D_6]-benzene, 25 ºC): δ = 32.5 (d, *J*(P,Rh) = 175 Hz, $PMePh_2$); $^{11}B\{^1H\}$ NMR (160.5 MHz, [D_6]-benzene, 25 ºC): δ = –1.56 (s, BH); HR-MS *m/z* calcd. for $C_{35}H_{37}BN_6P_2Rh$ [*M*+H]$^+$ 716.1624, found: 716.1625 (error (mD) = 0.1); anal. calcd. (%) for $C_{35}H_{36}N_6BP_6Rh$ (716.38): C 58.68, H 5.07, N 11.73; found: C 58.61, H 4.95, N 11.17.

Reaction of [Rh(Tp)(C_2H_4)($PHPh_2$)] (2) with PPh_3. An NMR tube was charged with equimolar amounts of complex **2** (15.9 mg, 0.03 mmol) and PPh_3 (7.9 mg, 0.03 mmol), [D_8]-toluene (0.5 mL) was added and the reaction was monitored by NMR. $^{31}P\{^1H\}$ NMR (161.3 MHz, [D_8]-toluene, –60 ºC) for [Rh(Tp)(H)(PPh_3)(PPh_2)] (**10a**) δ = 46.6 (dd, *J*(P,Rh) = 141, ^2J(P,P) = 12 Hz, 1P, PPh_3), 41.1 (dd, *J*(P,Rh) = 68, ^2J(P,P) = 12 Hz, 1P, PPh_2), for [Rh(κ^2-Tp)(PPh_3)($PHPh_2$)] (**10b**-Tp-in) δ = 54.0 (dd, *J*(P,Rh) = 169, ^2J(P,P) = 58 Hz, 1P, PPh_3), 28.5 (dd, *J*(P,Rh) = 171, ^2J(P,P) = 58 Hz, 1P, $PHPh_2$), for [Rh(κ^2-Tp)(PPh_3)($PHPh_2$)] (**10b**-Tp-out) δ = 54.6 (dd, *J*(P,Rh) = 168, ^2J(P,P) = 55 Hz, 1P, PPh_3), 32.0 (dd, *J*(P,Rh) = 171, ^2J(P,P) = 55 Hz, 1P, $PHPh_2$); ^{1}H NMR (400.13 MHz, [D_8]-toluene, 25 ºC) selected resonances: δ = –14.45 (ddd, ^2J(H,P) = 22.5, ^2J(H,P) = 6.6, *J*(H,Rh) = 13.4 Hz, 1H, Rh–H, **10a**), 5.38 (dd, ^1J(H,P) = 355.5 Hz, ^3J(H,Rh) = 16.1 Hz, 1H, $PHPh_2$, **10b**); $^{11}B\{^1H\}$ NMR (128.4 MHz, [D_8]-toluene, 25 ºC): δ = –3.90 (s, BH, 10a), –2.05 (s, BH, **10b**).

[Rh(Tp)(IMes)(PHPh$_2$)] (11). IMes (44.7 mg, 0.150 mmol) was added to a solution of [Rh(Tp)(C_2H_4)(PHPh$_2$)] (**2**, 77.8 mg, 0.150 mmol) in toluene (5 mL). After stirring for 30 min, the solution was concentrated to ca. 0.5 mL and layered with hexane (6 mL). The orange microcrystals that precipitated were separated by decantation, washed with hexane (2 mL) and vacuum-dried. Yield: 84 mg (71%). IR (ATR): ν(B–H)/cm^{-1} 2433 (m); ^{1}H NMR (400.13 MHz, [D$_6$]-benzene, 25 ºC): δ = 8.07 (br s, 1H, Pz^{A3}), 7.91 (br s, 1H, Pz^{A5}), 7.84 (d, ^3J(H,H) = 2.4 Hz, 1H, Pz^{C5}), 7.69 (d, ^3J(H,H) = 2.3 Hz, 1H, Pz^{B5}), 7.43 (br s, 1H, Pz^{B3}), 7.38 (br t, ^3J(H,H) = ^3J(H,P) = 8.6 Hz, 2H, HPPh^{o1}), 7.30 (m, 2H, HPPh^{o2}), 7.00 (br s, 4H, HPPh$^{m2+p1+p2}$), 6.91 (t, ^3J(H,H) = 7.2 Hz, HPPh^{m1}), 6.86 (s, 1H, Ar^A), 6.84 (s, 1H, Ar^B), 6.76 (d, ^3J(H,H) = 1.9 Hz, 1H, Pz^{C3}), 6.50 (br t, ^3J(H,H) = 1.8 Hz, Pz^{A4}), 6.43 (s, 1H, Ar^B), 6.39 (s, 1H, Ar^A), 6.23 (d, ^3J(H,H) = 1.9 Hz, Im^1), 6.19 (d, ^3J(H,H) = 1.9 Hz, Im^2), 5.95 (d, J(H,P) = 332.5 Hz, ^3J(H,Rh) = 3.3 Hz, 1H, PHPh$_2$), 5.87 (br t, 1H, Pz^{B4}), 5.47 (t, ^3J(H,H) = 2.2 Hz, 1H, Pz^{C4}), 3.05 (s, 3H, Me^{oA}), 2.23 (s, 3H, Me^{oB}), 2.23 (s, 3H, Me^{pB}), 2.04 (s, 3H, Me^{pA}), 2.00 (s, 3H, Me^{oA}), 1.59 (s, 3H, Me^{oB}); ^{31}P{^{1}H} NMR (162.0 MHz, [D$_6$]-benzene, 25 ºC): δ = 21.1 (d, J(P,Rh) = 195 Hz, 1P, HPPh$_2$); ^{11}B{^{1}H} NMR (128.4 MHz, [D$_6$]-benzene, 25 ºC): δ = –2.55 (s, BH); HR-MS *m/z* calcd. for $C_{42}H_{45}BN_8PRh$ [*M*]$^+$ 806.2654, found: 806.2691 (error (mD) = –3.7); anal. calcd. (%) for $C_{42}H_{45}N_8BPRh$ (806.55): C 62.54, H 5.62, N 13.89; found: C 62.91, H 5.52, N 13.28.

[Rh(Tp)(BzIMe)(PHPh$_2$)] (12) was prepared as described above for **10** starting from BzIMe (12.8 mg, 0.088 mmol) and [Rh(Tp)(C_2H_4)(PHPh$_2$)] (**2**, 46.4 mg, 0.088 mmol). Yield: 34.1 mg (60%). IR (ATR): ν(B–H)/cm^{-1} 2468 (m), ^{1}H NMR (400.13 MHz, [D$_8$]-toluene, 65 ºC): δ = 7.64 (d, ^3J(H,H) = 2.1 Hz, 3H, Pz^5), 7.36 (ddd, ^3J(H,P) = 11.1, ^3J(H,H) = 7.8, 1.7 Hz, 4H, HPPh^o), 7.26 (v br, 3H, Pz^3), 6.86 (m, 6H, HPPh^{m+p}), 6.81 (m, 2H) and 6.58 (m, 2H, A_2B_2 spin system, BzIm), 6.16 (dd, J(H,P) = 322.7, ^2J(H,Rh) = 1.1 Hz, 1H, HPPh$_2$), 6.02 (br s, 3H, Pz^4), 3.59 (s, 6H, Me); ^{31}P{^{1}H} NMR (162.0 MHz, [D$_8$]-toluene, 65 ºC): δ = 26.0 (d, J = 192 Hz, PHPh$_2$); ^{11}B{^{1}H} NMR (128.4 MHz, [D$_8$]-toluene, –50 ºC): δ = –1.93 (s, BH); HR-MS *m/z* calcd. for $C_{30}H_{30}BN_8PRh$ [*M*-H]$^+$ 647.1479, found: 647.1492 (error (mD) = –1.3); anal. calcd. (%) for $C_{30}H_{31}N_8BPRh$ (648.31): C 55.58, H 4.82, N 17.28; found: C 52.83, H 4.54, N 16.47.

[Rh(Tp)(η^1-Et)(κ^{C,P}-CH$_2$CH$_2$PPh$_2$)] (13). An NMR tube was charged with [Rh(Tp)(C_2H_4)(PHPh$_2$)] (**2**, 26.8 mg, 0.051 mmol) and benzene (0.6 mL) was added. The NMR tube was out under an ethylene atmosphere (6.0 bar) and the reaction mixture was heated at 60 °C for 6 days to give a cloudy light yellow solution. Then, toluene (2 mL) was added and the suspension was filtered off to remove small amounts of complex **3**. The filtrate was vacuum-dried, washed with hexane (2 x 0.5 mL) and vacuum-dried. Yield: 22.0 mg (78%). IR (ATR): ν(B-H)/cm^{-1} 2460 (m); ^{1}H NMR (500.13 MHz, [D$_6$]-benzene, 25 ºC): δ = 7.74 (d, ^3J(H,H) = 1.5 Hz, 1H, Pz^{A3}), 7.652 (d, ^3J(H,H)= 2.2 Hz, 2H, Pz^{C3}), 7.651 (d, ^3J(H,H) = 2.3 Hz, 1H, Pz^{A5}), 7.56 (dd, ^3J(H,H) = 2.3 Hz, ^4J(H,H) = 0.7 Hz, 1H, Pz^{B5}), 7.51 (ddd, ^3J(H,P) = 9.9 Hz, ^3J(H,H) = 7.5 Hz, ^4J(H,H) = 1.7 Hz, 2H, PPh^{o1}), 7.49 (d, ^3J(H,H) = 1.7 Hz, 1H, Pz^{C5}), 7.19 (dd, ^3J(H,P) = 10.6 Hz, ^3J(H,H) = 7.0 Hz, 2H, PPh^{o2}), 7.04 (m, 3H, PPh$^{(p+m)1}$), 6.87 (d, ^3J(H,H) = 1.5 Hz, 1H, Pz^{B3}), 6.84 (t, ^3J(H,H) = 7.5 Hz, 1H, PPh^{p2}), 6.71 (t, ^3J(H,H) = 6.9 Hz, 2H, PPh^{m2}), 6.09 (t, ^3J(H,H) = 2.1 Hz, 1H, Pz^{A4}), 5.94 (br, 1H, Pz^{C4}), 5.77 (t, ^3J(H,H) = 2.1 Hz, 1H, Pz^{B4}), 3.95 (dtd, ^2J(H,H) = 15.0 Hz, ^3J(H,H) = ^2J(H,P) = 10.9 Hz, ^3J(H,H) = 6.4 Hz, 1H, H^{3A}), 3.64 (dtd, ^2J(H,H) = 15.0 Hz, ^3J(H,H) = ^2J(H,P) = 10.6 Hz, ^3J(H,H) = 2.1 Hz, 1H, H^{3B}), 2.23 (pd, ^3J(H,H) = ^2J(H,Rh) = 7.8 z, ^2J(H,H) = 3.8 Hz, 1H, H^{1B}), 2.00 (pd, ^3J(H,H) = ^2J(H,Rh) =7.7, ^2J(H,H) = 3.8 Hz, 1H, H^{1A}), 1.72 (dddd, ^3J(H,P) = 14.0 Hz, ^3J(H,H) = 10.4 Hz, ^2J(H,Rh) =6.9 Hz, ^3J(H,H) = 3.9 Hz, 1H, H^{2B}), 1.41 (dddd, ^3J(H,P) = 13.3 Hz, ^3J(H,H) =10.8 Hz, ^2J(H,Rh) = 7.8 Hz, ^3J(H,H) = 2.7 Hz, 1H, H^{2A}), 1.00 (t, ^3J(H,H) = 7.8 Hz, 3H, Me); ^{31}P{^{1}H} NMR (202.5 MHz, [D$_6$]-benzene, 25 ºC): δ = –36.1 (d, J(P,Rh) = 122 Hz, 1P, PPh$_2$); ^{13}C{^{1}H}-apt NMR (125.8 MHz, [D$_6$]-benzene, 25 ºC), selected resonances: δ = 36.04 (dd, J(C,P) = 32 Hz, J(C,Rh) = 4 Hz, C^3) 18.2 (Me), 11.8 (dd, J(C,Rh) = 24 Hz, J(C,P) = 11 Hz, C^1), –9.46 (d, J(C,P) = 38 Hz J(C,Rh) = 20 Hz, C^2); ^{11}B{^{1}H} NMR (160.5 MHz, [D$_6$]-benzene, 25 ºC): δ = –3.52 (s, BH); (s); MS (*m/z* (%)): 558.2 (100) [*M*]$^+$; anal. calcd. (%) for $C_{25}H_{29}N_6BPRh$ (558.23): C 53.79, H 5.24, N 15.05; found: C 52.47, H 5.09, N 15.00.

[Rh(Tp)(H)(POPh$_2$)(PHPh$_2$)] (14). Diphenylphosphane oxide, (42.7 mg, 0.211 mmol) was added to a yellow solution of [Rh(Tp)(C_2H_4)(HPPh$_2$)] (**2**, 112.0 mg, 0.211 mmol) in toluene (3 mL) to produce an immediate color change to pale yellow. After stirring for 10 min, the solution was concentrated to ca. 0.5 mL, layered with hexane (6 mL) and left undisturbed for two days. The yellow microcrystals that precipitated were decanted, washed with cold hexane (1 x 2 mL) and vacuum-dried. Yield: 135.2 mg (91 %). IR (ATR): ν(B-H)/cm^{-1} 2464 (m), ν(Rh-H)/cm^{-1} 2114 (m); ^{1}H NMR (500.13 MHz, [D$_6$]-benzene, 25 ºC): δ = 8.52 (dd, ^3J(H,P) = 10.7 Hz, ^3J(H,H) = 7.1 Hz, 2H, POPh^{o1}), 8.36 (d, ^3J(H,H) = 1.9 Hz, 1H, Pz^{B3}), 7.61 (m, 2H, PPh^{o1}), 7.58 (d, ^3J(H,H) = 2.3 Hz, 1H, Pz^{B5}), 7.39 (d, ^3J(H,H) = 2.6 Hz, 1H, Pz^{C5}), 7.35 (td, ^3J(H,H) = 7.6 Hz, ^4J(H,P) = 2.1 Hz, 2H, POPh^{m1}), 7.29 (d, ^3J(H,H) = 2.2 Hz, 1H, Pz^{A5}), 7.22 (ddt, ^3J(H,H) = 8.8, ^4J(H,H) = 6.8 Hz, ^5J(H,P) = 1.5 Hz, 1H, POPh^{p1}), 7.17 (dd, J(H,P) = 410.2 Hz, ^2J(H,P) = 10.5 Hz, 1H, PHPh$_2$), 7.09 (m, 4H, POPh^{o2} + PPh^{o2}), 6.99 (d, ^3J(H,H) = 2.0 Hz, 1H, Pz^{A3}), 6.95 (m, 3H, PPh$^{(m+p)1}$), 6.88 (td, ^3J(H,H) = 7.4 Hz, ^4J(H,H) = 1.9 Hz, 1H, PPh^{p2}), 6.78 (m, 6H, POPh$^{(m+p)2}$ + PPh^{m2}), 6.77 (d, ^3J(H,H) = 1.9 Hz, 1H, Pz^{C3}), 5.87 (t, ^3J(H,H) = 2.1 Hz, 1H, Pz^{B4}), 5.62 (td, ^3J(H,H) = 2.2 Hz, ^5J(H,P) = 1.0 Hz, 1H, Pz^{C4}), 5.52 (td, ^3J(H,H) = 1.8 Hz, ^5J(H,P) = 0.9 Hz, 1H, Pz^{A4}), –13.73 (ddd, ^2J(H,P) = 23.2 Hz, 20.3 Hz, ^1J(H,Rh) = 16.2 Hz, 1H, Rh-H); ^{31}P{^{1}H} NMR (202.5 MHz, [D$_6$]-benzene, 25 ºC): δ = 75.7 (dd, ^1J(P,Rh) = 105 Hz, ^2J(P,P) = 40 Hz, 1P, OPPh$_2$), 33.5 (dd, ^1J(P,Rh) = 140 Hz, ^2J(P,P) = 40 Hz, 1P, PPh$_2$); ^{11}B{^{1}H} NMR (160.5 MHz, [D$_6$]-benzene, 25 ºC): δ = –3.68 (s, BH); HR-MS *m/z* calcd. for $C_{33}H_{33}N_6BOP_2Rh$ [*M*+H]$^+$ 705.1339, found 705.1332 (error (mD) = –0.7); anal. calcd. (%) for $C_{33}H_{32}N_6BOP_2Rh$ (704.31): C 56.28, H 4.58, N 11.93; found: 56.54, H 4.74, N 11.80.

[{(Tp)(η^1-Et)Rh(μ-OPPh$_2$)}$_2$] (15). A solution of OPHPh$_2$ (61.3 mg, 0.303 mmol) in toluene (5 mL) was dropwise added over 45 min to a yellow solution of [Rh(Tp)(C_2H_4)$_2$] (**1**, 112.9 mg, 0.303 mmol) in toluene (7 mL). The resulting pale-yellow solution was evaporated to dryness and the residue washed with acetone (3 x 1 mL) and vacuum-dried. Yield: 75.3 mg (46 %). IR (ATR): ν(B-H)/cm^{-1} 2485 (m); ^{1}H NMR (400.13 MHz, [D$_6$]-benzene, 25 ºC): δ = 8.02 (d, ^3J(H,H) = 2.1 Hz, 1H, Pz^{A3}), 8.00 (m, 2H, POPh^{o1}), 7.57 (dd, ^3J(H,H) = 2.3 Hz, ^4J(H,H) = 0.6 Hz, 1H, Pz^{B5}), 7.46 (dd, ^3J(H,H) = 2.5 Hz, ^4J(H,H) = 0.8 Hz, 1H, Pz^{C5}), 7.38 (d, ^3J(H,H) = 2.3 Hz, 1H, Pz^{A5}), 7.20 (t, ^3J(H,H) = 7.1 Hz, 2H, POPh^{m1}), 7.16 (overlapped, 1H, Pz^{B3}), 7.14 (m, 3H, POPh^{o2} + POPh^{p1}), 6.99 (d, ^3J(H,H) = 2.2 Hz, 1H, Pz^{C3}), 6.79 (ddd, ^3J(H,H) = 8.8, 6.0 Hz, ^4J(H,H) = 1.4 Hz, 1H, POPh^{p2}), 6.61 (t, ^3J(H,H) = 7.3 Hz, 2H, POPh^{m2}), 5.75 (td, ^3J(H,H) = 2.1 Hz, ^5J(H,P) = 1.1 Hz, 1H, Pz^{A4}), 5.71 (t, ^3J(H,H) = 2.3 Hz, 1H, Pz^{C4}), 5.67 (t, ^3J(H,H) = 2.1 Hz, 1H, Pz^{B4}), 4.64 (p, ^3J(H,H) = ^2J(H,H) = 8.7 Hz, 1H, CH$_2$), 3.17 (h, ^3J(H,H) = ^2J(H,H) = ^3J(H,P) = 8.7 Hz, 1H, CH$_2$), 1.15 (t, ^3J(H,H) = 7.5 Hz, 3H, Me); ^{31}P{^{1}H} NMR (162.0 MHz, [D$_6$]-benzene, 25 ºC): δ = 91.4 (m, AA' part of a AA'XX' spin system (A = ^{31}P, X = ^{103}Rh), OPPh$_2$); Selected ^{13}C resonances from the ^{1}H,^{13}C-hsqc spectrum, δ = 20.1 (CH$_2$), 18.1 (Me); ^{11}B{^{1}H} NMR (128.8 MHz, [D$_6$]-benzene, 25 ºC): δ = –3.1 (s, BH); HR-MS *m/z* calcd. for $C_{23}H_{25}BN_6PORh$ [*M/2+H*]$^+$ 547.1052, found: 547.1012 (error (mD) = 4.0); Anal. Calcd (%) for $C_{46}H_{50}N_{12}B_2O_2P_2Rh_2$ (1092.35): C 50.58, H 4.61, N 15.39; found: C 49.94, H 4.72, N 15.16.

[Rh(Tp)(η^1-R)(POPh$_2$)(POHPh$_2$)] (R = Et, 16 and H, 17). Diphenylphosphane oxide, (42.7 mg, 0.211 mmol) was added to a cloudy yellow suspension of [{(Tp)(η^1-Et)Rh(μ-OPPh$_2$)}$_2$] (**15**, 46.0 mg, 0.042 mmol) in toluene (6 mL). After stirring for 14 hours at 60˚C, the light yellow solution was evaporated and the residue was crashed with hexane (5 mL). Afterthat, the resulting white solid was washed with

hexane (2 x 1mL) and vacuum-dried. Yield: 60.9 mg (98 %, ratio **16**:**17** = 2:1).

NMR data for [Rh(Tp)(η^1-Et)($POPh_2$)($POHPh_2$)] (**16**, 66.6%): ^{1}H NMR (500.13 MHz, [D_6]-benzene, 25 ºC): δ = 18.34 (br s, 1H, POH), 7.92 (dddd, ^3J(H,H) = 7.9 Hz, ^3J(H,P) = 5.7, ^4J(H,H) = 3.7 Hz, ^4J(H,H) = 1.6 Hz, 4H, $POPh^{o1}$), 7.55 (d, ^3J(H,H) = 2.3 Hz, 4H, $Pz^{A3,A5}$), 7.36 (d, ^3J(H,H) = 2.3 Hz, 1H, Pz^{B5}), 7.12 (m, 4H, $POPh^{m1}$), 7.09 (m, 2H, $POPh^{p1}$), 6.91 (dddd, ^3J(H,H) = 6.8 Hz, ^3J(H,P) = 5.2, ^4J(H,H) = 3.8 Hz, ^4J(H,H) = 1.4 Hz, 4H, $POPh^{o2}$), 6.83 (m, 4H, $POPh^{m2}$), 6.75 (m, 2H, $POPh^{p2}$), 6.74 (d, ^3J(H,H) = 2.3 Hz, 1H, Pz^{B3}), 5.84 (t, ^3J(H,H) = 2.2 Hz, 1H, Pz^{A4}), 5.21 (t, ^3J(H,H) = 2.1 Hz, 1H, Pz^{B4}), 2.22 (qtd, ^3J(H,H) = 7.5 Hz, ^3J(H,P) = 4.1 Hz, ^2J(H,Rh) = 1.9 Hz, 2H, CH_2), 0.52 (t, ^3J(H,H) = 7.5 Hz, 3H, Me); $^{31}P\{^1H\}$ NMR (202.5 MHz, [D_6]-benzene, 25 ºC): δ = 88.2 (d, J(P,Rh) = 140 Hz, 2P); $^{11}B\{^1H\}$ NMR (160.5 MHz, [D_6]-benzene, 25 ºC): δ = –4.24 (s, BH).

NMR data for [Rh(Tp)(H)($POPh_2$)($POHPh_2$)] (**17**, 33.3%): ^{1}H NMR (500.13 MHz, [D_6]-benzene, 25 ºC): δ = 18.34 (br s, 1H, POH), 8.18 (dddd, ^3J(H,H) = 7.1 Hz, ^3J(H,P) = 5.9, ^4J(H,H) = 3.9 Hz, ^4J(H,H) = 2.1 Hz, 4H, $POPh^{o1}$), 7.42 (d, ^3J(H,H) = 2.3 Hz, 1H, Pz^{B5}), 7.33 (d, ^3J(H,H) = 2.5 Hz, 1H, Pz^{A5}), 7.12 (m, 4H, $POPh^{o2}$), 7.10 (m, 1H, Pz^{B3}), 7.09 (m, 4H, $POPh^{m1}$), 7.08 (m, 2H, $POPh^{p1}$), 6.80 (m, 2H, $POPh^{p2}$), 6.76 (m, 4H, $POPh^{m2}$), 6.68 (d, ^3J(H,H) = 2.0 Hz, 1H, Pz^{A3}), 5.54 (t, ^3J(H,H) = 2.3 Hz, 1H, Pz^{A4}), 5.52 (t, ^3J(H,H) = 2.2 Hz, 1H, Pz^{B4}), –12.99 (td, ^2J(H,P) = 21.7 Hz, J(H,Rh) = 16.7 Hz, 1H, Rh–H); $^{31}P\{^1H\}$ NMR (202.5 MHz, [D_6]-benzene, 25 ºC): δ = 97.3 (d, J(P,Rh) = 128 Hz, 2P); $^{11}B\{^1H\}$ NMR (160.5 MHz, [D_6]-benzene, 25 ºC): δ = –4.24 (s, BH).

DFT geometry optimizations. The DFT geometry optimizations and thermochemical calculations were carried out with the Gaussian 09 program package,[51] using the B3LYP-D3 hybrid functional.[52] Geometry optimizations were performed in the gas phase with the LanL2TZ(f) effective core potential basis set for the metal atoms, and the 6-311G(d,p) basis set for the remaining ones.

Profiles for reactions in Figures 8-10 were computed with the Turbomole program[53] coupled to the PQS Baker optimizer[54] via the BOpt package.[55] Geometries were fully optimized as minima or transition states using the BP86 functional,[56] the Turbomole def2-TZVP basis set[57] and a small grid size (m4). To reduce computation time, the resolution-of-identity (ri) approximation[58] was applied. Grimme's dispersion corrections (version D3, disp3, 'zero damping)' were applied to include Van der Waals interactions.[59]

X-ray diffraction studies on complexes [(Tp)(H)Rh(μ-PPh_2)$_2$Rh($PHPh_2$)$_2$] 0.5H_2O (7·0.5H_2O), [Rh(Tp)(IMes)($PHPh_2$)] (11) and [Rh(Tp)(H)($POPh_2$)($PHPh_2$)] (14). Intensity measurements were collected with a Bruker Smart Apex-II (**7** and **11**) or a Bruker Smart Apex (**14**) diffractometers, with graphite-monochromated $Mo_{K\alpha}$ radiation at 100 K (ω scans of 0.3º). A semi-empirical absorption correction was applied to the data set with the multi-scan[60] methods. The structures were solved by direct methods with SHELXS-2013[61] (**7** and **14**) or SHELXT-2014[62] (**11**) and refined by full-matrix least-squares on F^2 with the program SHELXL-2016,[63] in the WINGX[64] package. In the 24.7(14)% of the crystal of **14** the phosphanido and the phosphane oxide ligands are swapped. All non-hydrogen atoms were refined with anisotropic displacement parameters, and their hydrogen atoms were geometrically calculated and refined by the riding mode, including the isotropic displacement parameters The hydride ligands were located in difference-Fourier maps and refined with a geometrical restraint (DFIX card). The hydrogens bonded to phosphorus (**7** and **11**) or boron atoms (**7**) were also located in a difference-Fourier map and refined with some degree of freedom. Hydrogen atoms of the water solvent (**7**) were not included in the model. For selected crystallographic data see the Supporting Information.

CCDC 1949932 (**7**·0.5H_2O), 1949933 (**11**) and 1949934 (**14**) contain the supplementary crystallographic data for this paper. These data can be obtained free of charge from The Cambridge Crystallographic Data Centre via www.ccdc.cam.ac.uk/data_request/cif.

Acknowledgements

The generous financial support from AEI/FEDER, UE (CTQ2017-83421-P, C.T.), Gobierno de Aragón/FEDER (GA/FEDER, Inorganic Molecular Architecture Group E08_17R; C.T.) and the Netherlands Organization for Scientific Research (NWO) (TOP Grant 716.015.001, B.dB) is gratefully acknowledged. V.V. thanks MINECO/FEDER for a FPI fellowship. The 'Centro de Supercomputación de Galicia (CESGA)' is also gratefully acknowledged for generous allocation of time.

Keywords: P–H activation • Rhodium • Oxidative Addition • Insertion • rhodaphosphacyclobutane

[1] *See for example*: a) S. Bezzenine-Lafollée, R. Gil, D. Prim, J. Hannedouche, *Molecules* **2017**, *22*, 1901; b) C. A. Bange, R. Waterman, *Chem. Eur. J.* **2016,** *22*, 12598–12605; c) A. A. Trifonov, I. V. Basalov, A. A. Kissel, *Dalton Trans.* **2016**, *45*, 19172–19193; d) V. Koshti, S. Gaikwad, S. H. Chikkali, *Coord. Chem. Rev.* **2014,** *265*, 52–73; e) P. E. Sues, A. J. Lough, R. H. Morris, *J. Am. Chem. Soc.* **2014**, *136*, 4746–4760 *and references therein*; f) L. Rosenberg, *ACS Catal.* **2013**, *3*, 2845–2855; g) R. Waterman, *Chem. Soc. Rev.* **2013**, *42*, 5629–5641; h) V. P. Ananikov, I. P. Beletskaya, *Top. Organomet. Chem.* **2013**, *43*, 1–20; i) E. M. Leitao, T. Jurca, I. Manners, *Nat. Chem.* **2013**, *5*, 817–829; j) R. Waterman, *Curr. Org, Chem.* **2012**, *16*, 1313–1331; k) D. S. Glueck, *Top. Organomet. Chem.* **2010**, *31*, 65–100; l) S. Greenberg, D. W. Stephan, *Chem. Soc. Rev.* **2008**, *37*, 1482–1489; m) T. J. Clark, K. Lee, I. Manners, *Chem. Eur. J.* **2006**, *12*, 8634–8648; n) C. A. Jaska, A. Bartole-Scott, I. Manners, *Dalton Trans.* **2003**, 4015–4021.

[2] a) R. Waterman, *Dalton Trans.* **2009**, 18–26; b) D. S. Glueck, *Dalton Trans.* **2008**, 5276–5286.

[3] T. Chen, C.-Q. Zhao, L.-B. Han, *J. Am. Chem. Soc.* **2018**, *140*, 3139–3155.

[4] Y. Xu, Z. Yang, B. Ding, D. Liu, Y. Liu, M. Sugiya, T. Imamoto, W. Zhang, *Tetrahedron* **2015**, *71*, 6832–6839.

[5] S. K. Gibbons, Z. Xu, R. P. Hughes, D. S. Glueck, A. L. Rheingold, *Organometallics* **2018**, *37*, 2159–2166.

[6] R. L. Webster, *Inorganics* **2018**, *6*, 120.

[7] a) A. K. King, K. J. Gallagher, M. F. Mahon, R. L. Webster, *Chem. Eur. J.* **2017**, *23*, 9039–9043; b) M. Espinal-Viguri, A. K. King, J. P. Lowe, M. F. Mahon, R. L. Webster, *ACS Catal.* **2016**, *6*, 7892−7897; c) A. K. King, A. Buchard, M. F. Mahon, R. L. Webster, *Chem. Eur. J.* **2015**, *21*, 15960–15963.

[8] a) A. N. Selikhov, T. V. Mahrova, A. V. Cherkasov, G. K. Fukin, E. Kirillov, C. A. Lamsfus, L. Maron, A. A. Trifonov, *Organometallics* **2016**, *35*, 2401–2409; b) W. Ma, L. Xu, W.-X. Zhang, Z. Xi, *New J. Chem.* **2015**, *39*, 7649–7655; c) A. C. Behrle, L. Castro, L. Maron, R. Walensky, *J. Am. Chem. Soc.* **2015**, *137*, 14846–14849; d) A. C. Behrle, J. A. R. Schmidt, *Organometallics* **2013**, *32*, 1141–1149; e) W.-X. Zhang, M. Nishiura, T. Mashiko, Z. Hou, *Chem. Eur. J.* **2008**, *14,*

2167–2179; f) M. R. Douglass, T. J. Marks, *J. Am. Chem. Soc.* **2000**, *122,* 1824–1825.

[9] a) J. Yuan, H. Hu, C. Cui, *Chem. Eur. J.* **2016**, *22*, 5778–5785; b) X. Gu, L. Zhang, X. Zhu, S. Wang, S. Zhou, Y. Wei, G. Zhang, X. Mu, Z. Huang, D. Hong, F. Zhang, *Organometallics* **2015**, *34*, 4553–4559.

[10] a) R. Waterman, *Organometallics* **2007**, *26,* 2492–2494; b) M. Driess, J. Aust, K. Merz, *Eur. J. Inorg. Chem.* **2002**, 2961–2964.

[11] J. Li, C. A. Lamsfus, C. Song, J. Liu, G. Fan, L. Maron, C. Cui, *ChemCatChem* **2017**, *9*, 1368–1372.

[12] a) K.-S. Feichtner, V. H. Gessner, *Chem. Commun.* **2018**, *54*, 6540–6553; b) J. Weismann, L. T. Scharf, V. H. Gessner, *Organometallics* **2016**, *35*, 2507–2515.

[13] a) X. Qi, H. Zhao, H. Sun, X. Li, O. Fuhr, D. Fenske, *New J. Chem.* **2018**, *42*, 16583–16590; b) C. Martin, S. Mallet-Ladeira, K. Miqueu, G. Bouhadir, D. Bourissou, *Organometallics* **2014**, *33*, 571–577; c) E. J. Derrah, C. Martin, S. Mallet-Ladeira, K. Miqueu, G. Bouhadir, D. Bourissou, *Organometallics* **2013**, *32*, 1121–1128.

[14] Y. Gloaguen, W. Jacobs, B. de Bruin, M. Lutz, J. I. van der Vlugt, *Inorg. Chem.* **2013**, *52*, 1682–1684.

[15] R. A. Schunn, *Inorg. Chem.* **1973**, *12*, 1573–1579.

[16] a) E. A. V. Ebsworth, R. A. Mayo, *J. Chem. Soc. Dalton Trans.* **1988**, 477–484; b) E. A. V. Ebsworth, R. O. Gould, R. A. Mayo, M. Walkinshaw, *J. Chem. Soc. Dalton Trans.* **1987**, 2831–2838; c) E. A. V. Ebsworth, R. Mayo, *Angew. Chem.* **1985**, *97*, 65–66; *Angew. Chem. Int. Ed. Engl.* **1985**, *24*, 68–70.

[17] a) A. L. Serrano, M. A. Casado, M. A. Ciriano, B. de Bruin, J. A. López, C. Tejel*, Inorg. Chem.* **2016**, *55*, 828–839; b) I. Mena, M. A. Casado, V. Polo, P. García-Orduña, F. J. Lahoz, L. A. Oro, *Dalton Trans.* **2014**, *43*, 1609–1619.

[18] a) I. Kovacik, D. K. Wicht, N. S. Grewal, D. S. Glueck, C. D. Incarvito, I. A. Guzei, A. L. Rheingold, *Organometallics* **2000**, *19*, 950–953; b) I. V. Kourkine, M. D. Sargent, D. S. Glueck, *Organometallics* **1998**, *17*, 125–127; c) D. K. Wicht, I. V. Kourkine, B. M. Lew, J. M. Nthenge, D. S. Glueck, *J. Am. Chem. Soc.* **1997**, *119,* 5039–5040.

[19] Y. S. Ganushevich, V. A. Miluykov, F. M. Polyancev, S K. Latypov, P. Lönnecke, E. Hey-Hawkins, D. G. Yakhvarov, O. G. Sinyashin, *Organometallics* **2013**, *32*, 3914–3919.

[20] G. Bai, P. Wei, A. K. Das, D. W. Stephan, *Dalton Trans.* **2006**, 1141–1146.

[21] a) M. Itazaki, Y. Nishihara, K. Osakada, *Organometallics* **2004**, *23,* 1610–1621.

[22] D. Wang, Q. Chen, X. Leng, L. Deng, *Inorg. Chem.* **2018**, *57*, 15600−15609.

[23] J. B. Bonanno, P. T. Wolczanski, E. B. Lobkovsky, *J. Am. Chem. Soc.* **1994**, *116*, 11159–11160.

[24] R. T. Baker, J. C. Calabrese, R. L. Harlow, I. D. Williams, *Organometallics* **1993**, *12*, 830–841.

[25] L. D. Field, N. G. Jones, P. Turner, *J. Organomet. Chem.* **1998**, *571*, 195–199.

[26] L.-B. Han, T. D. Tilley, *J. Am. Chem. Soc.* **2006**, *128*, 13698–13699.

[27] V. P. W. Böhm, M. Brookhart, *Angew. Chem.* **2001**, *113*, 4832–4834; *Angew. Chem. Int. Ed.* **2001**, *40*, 4694–4696.

[28] U. Fischbach, M. Trincado, H. Grützmacher, *Dalton Trans.* **2017**, *46*, 3443–3448.

[29] A. M. Geer, A. L. Serrano, B. de Bruin, M. A. Ciriano, C. Tejel, *Angew. Chem.* **2015**, *127*, 482–485; *Angew. Chem. Int. Ed.* **2015**, *54*, 472–475.

[30] a) R. Shimogawa, Y. Tsurumaki, T. Kuzutani, T. Takao, *Organometallics* **2018**, *37*, 290–293; b) G. Luo, Y. Luo, Z. Hou, *Organometallics* **2017**, *36*, 4611–4619; c) M. P. Shaver, M. D. Fryzuk, *Organometallics* **2005,** *24,* 1419–1427.

[31] W. C. Fultz, A. L. Rheingold, P. E. Kretrer, D. W. Meek, *Inorg. Chem.* **1983***, 22*, 860–863.

[32] *See for example*: a) D. O. Downing, P. Zavalij, B. W. Eichhorn, *Inorg. Chim. Acta* **2011**, *375*, 329–332; b) C. Tejel, M. Sommovigo, M. A. Ciriano, J. A. López, F. J. Lahoz, L. A. Oro, *Angew. Chem.* **2000**, *112*, 2426–2429; *Angew. Chem. Int. Ed.* **2000**, *39*, 2336–2339; c) K. Wang, T. J. Emge, A. S. Goldman, *Inorg. Chim. Acta* **1997**, *255*, 395–398; d) A. M. Arif, R. A. Jones, M. H. Seeberger, B. R. Whittlesey, T. C. Wright, *Inorg. Chem.* **1986**, *25*, 3943–3949; e) E. W. Burkhardt, W. C. Mercer, G. L. Geoffroy *Inorg. Chem.* **1984**, *23*, 1779–1782; f) P. E. Kreter, D. W. Meek, *Inorg. Chem.* **1983**, *22*, 319–326; g) R. A. Jones, T. C. Wright, J. L. Atwood, W. E. Hunter, *Organometallics* **1983**, *2*, 470–472.

[33] a) J. Kadis, Y. K. Shin, J. I. Dulebohn, D. L. Ward, D. G. Nocera, *Inorg. Chem.* **1996**, *35*, 811–817; b) J. I. Dulebohn, D.L. Ward, D. G. Nocera, *J. Am. Chem. Soc.* **1988**, *110*, 4054–4056.

[34] a) D. W. Meek, P. E. Kreter, G. G. Christoph, *J. Organomet. Chem.* **1982**, *231*, C53–C58; b) S. K Kang, T. A. Albright, T. C. Wright, R. A. Jones, *Organometallics* **1985**, *4*, 666-675.

[35] Complexes [Rh(acac)(L)(CO)] were prepared in situ by addition of the appropriate ligand to solutions of [Rh(acac)$(CO)_2$] in toluene. The related [Rh(Tp)(L)(CO)] complexes were not used in this study since the κ^2-κ^3 isomerism complicate the IR spectra.

[36] a) D. G. Gusev, *Organometallics* **2009**, *28,* 763–770; b) D. G. Gusev, *Organometallics* **2009**, *28*, 6458–6461.

[37] J. A. Bilbrey, A. H. Kazez, J. Locklin, W. D. Allen, *J. Comput. Chem.* **2013**, *34*, 1189–1197.

[38] C. Slugovc, I. Padilla-Martínez, S. Sirol, E. Carmona, *Coord. Chem. Rev.* **2001**, *213*, 129–157.

[39] M. Paneque, P. J. Pérez, A. Pizzano, M. L. Poveda, S. Taboada, M. Trujillo, E. Carmona, *Organometallics* **1999**, *18,* 4304–4310.

[40] P. E. Garrou, *Chem. Rev.* **1981**, *81,* 229–266.

[41] a) K. M. E. Burton, D. A. Pantazis, R. G. Belli, R. McDonald, L. Rosenberg, *Organometallics* **2016,** *35*, 3970–3980; b) R. G. Belli, K. M. E. Burton, S. A. Rufh, R. McDonald, L. Rosenberg, *Organometallics* **2015,** *34*, 5637–5646; c) E. J. Derrah, R. McDonald, L. Rosenberg, *Chem. Commun.* **2010**, *46*, 4592–4594; d) E. J. Derrah, D. A. Pantazis, R. McDonald, L. Rosenberg, *Angew. Chem.* **2010***, 122,* 3439–3442*; Angew. Chem. Int. Ed.* **2010,** *49*, 3367–3370.

[42] H. Geissler, P. Gross, B. Guckes, New pallada-phospha-cyclobutane compounds obtained by reacting special tri:organyl-phosphane compounds with palladium salts, palladium complexes or alkali palladate salts in organic solvent, Patent number: DE19647584-A1, 20 May 1998

[43] a) E. Igartúa-Nieves, A. J. Rivera-Brown, J. E. Cortés-Figueroa, *Inorg. Chem. Commun.* **2012,** *21*, 43–46; b) C. Cao, T. Wang, B. O. Patrick, J. A. Love, *Organometallics* **2006,** *25*, 1321–1324; c) M. A. Bennett, S. K. Bhargava, M. Ke, A. C. Willis, *J. Chem. Soc. Dalton Trans.* **2000**, 3537–3545.

[44] R. Waterman, G. L. Hillhouse, *J. Am. Chem. Soc.* **2003**, *125*, 13350–13351.

[45] For a first order reaction ($\ln\frac{[A]^t}{[A]^0} = -kt$) reaching 99% conversion in 6 days, the rate constant k is approx. 8.9x10^{-6} s^{-1}, which translates to a free energy barrier $\Delta G^{\ddagger}$ of approx. +27.3 kcal mol^{-1} using the Eyring–Polanyi equation ($k = \frac{k_B T}{h} e^{-\frac{\Delta G^{\ddagger}}{RT}}$, with k_B = Boltzmann constant, R = gas constant, h = Planck constant and assuming a transmission coefficient of 1).

[46] a) V. P. Ananikov, A. V. Makarov, I. P. Beletskaya, *Chem. Eur. J.* **2011**, *17*, 12623–12630; b) V. P. Ananikov, I. P. Beletskaya, *Chem. Asian J.* **2011**, *6*, 1423–1430.

[47] 2.6 kcal mol^{-1} (DFT-gas phase): A. Christiansen, C. Li, M. Garland, D. Selent, R. Ludwig, A. Spannenberg, W. Baumann, R. Franke, A. Börner, *Eur. J. Org. Chem.* **2010**, 2733–2741.

[48] J. A. López, private communication.

[49] A. M. Geer, J. A. López, M. A. Ciriano, C. Tejel, *Organometallics* **2016**, *35*, 799–808, *and references therein*.

[50] S. Trofimenko, *J. Am. Chem. Soc.* **1969**, *91*, 588–595.

[51] See the Supporting Information for a complete reference.

[52] a) C. Lee, W. Yang, R. G. Parr, *Phys. Rev. B* **1988**, *37*, 785–789; b) A. D. Becke, *J. Chem. Phys.* **1993**, *98*, 1372–1377; c) A. D. Becke, *J. Chem. Phys.* **1993**, *98*, 5648–5652; d) S. Grimme, J. Antony, S. Ehrlich, Krieg, H. J. *Chem. Phys.* **2010**, *132*, 154104.

[53] University of Karlsruhe and Forschungszentrum Karlsruhe GmbH. *TURBOMOLE* V7.3.1; TURBOMOLE GmbH, 2018.

[54] J. Baker *J. Comput. Chem.* **1986**, *7*, 385.

[55] P. H. M. Budzelaar, *J. Comput. Chem.* **2007**, *28*, 2226.

[56] a) J. P. Perdew *Phys. Rev. B: Condens. Matter Mater. Phys.* **1986**, *33*, 8822; b) A.D. Becke *Phys. Rev. A: At., Mol., Opt. Phys.* **1988**, *38*, 3098.

[57] F. Weigend, R. Ahlrichs *Phys. Chem. Chem. Phys.* **2005**, *7*, 3297.

[58] a) K. Eichkorn, F. Weigend, O. Treutler, R. Ahlrichs *Theor. Chem. Acc.* **1997**, *97*, 119; b) K. Eichkorn, O. Treutler, H. Öhm, M. Häser, R. Ahlrichs *Chem. Phys. Lett.* **1995**, *240*, 283; c) F. Weigend, *Phys. Chem. Chem. Phys.* 2006, 8, 1057.

[59] S. Grimme, J. Antony, S. Ehrlich, H. Krieg *J. Chem. Phys.* **2010**, *132*, 154104.

[60] G. M. Sheldrick, SADABS, Bruker AXS, Madison, WI (USA), 1997.

[61] G. M. Sheldrick, *Acta Cryst.* **2008**, *A64*,112–122.

[62] G. M. Sheldrick, *Acta Cryst.* **2015**, *A71*, 3–8.

[63] G. M. Sheldrick, *Acta Cryst.* **2015**, *C71*, 3–8.

[64] L. J. Farrugia, *J. Appl. Crystallogr.* **2012**, *45*, 849–854.

10.1002/chem.201903981

WILEY-VCH

Entry for the Table of Contents (Please choose one layout)

Layout 1:

FULL PAPER

Combination of tridentate hydrido-tris(pyrazolyl)borate and phosphane ligands on rhodium provides a useful platform for the selective oxidative-addition reaction of P–H bonds, ethylene insertion reactions into Rh–H bonds as well as P–C bond formation reactions of non-activated olefins such as ethylene.

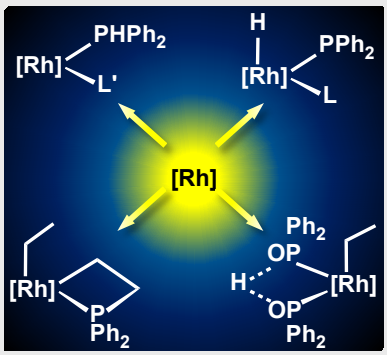

Víctor Varela-Izquierdo, Ana Mª Geer, Bas de Bruin, José A. López, Miguel A. Ciriano, and Cristina Tejel**

Page No. – Page No.

Rhodium Complexes in P–H Bond Activation Reactions

Layout 2:

FULL PAPER

((Insert TOC Graphic here; max. width: 11.5 cm; max. height: 2.5 cm))

Page No. – Page No.

Title

Text for Table of Contents